11
Planetary Waves, Wave Drag and Meridional Transport

"Profound ideas grow out of simple models…always remember to think deeply of simple things"

R.T. Pierrehumbert, *Principles of Planetary Climate*. Cambridge University Press, 2010, page 628.

11.1 Introduction

This chapter continues the discussion of zonal mean state of the atmosphere that was started in chapter 7 and continued at the end of **chapter 10**. Here we focus especially on the quasi-geostrophic interpretation of the role of large scale baroclinic eddies and planetary waves in determining the zonal mean meridional circulation in the mid-latitudes and in altering the zonal mean zonal flow, a topic that is referred to as "**wave-mean flow interaction**".

The meandering of the jet in middle latitudes around the hemisphere is determined mainly by mountains, by thermal contrasts between land and sea, by baroclinic instability in the troposphere and by potential vorticity sources and sinks due to latent heat release in large-scale precipitation systems. In other words, the wave sources are located exclusively at the Earth's surface or in the troposphere. This leads to a Rossby wave-pattern in the troposphere with quite a lot of variability in it. This fact is illustrated in the Hövmoller diagrams of the meridional wind, averaged between 40°N and 60°N, shown in **figure 11.1**

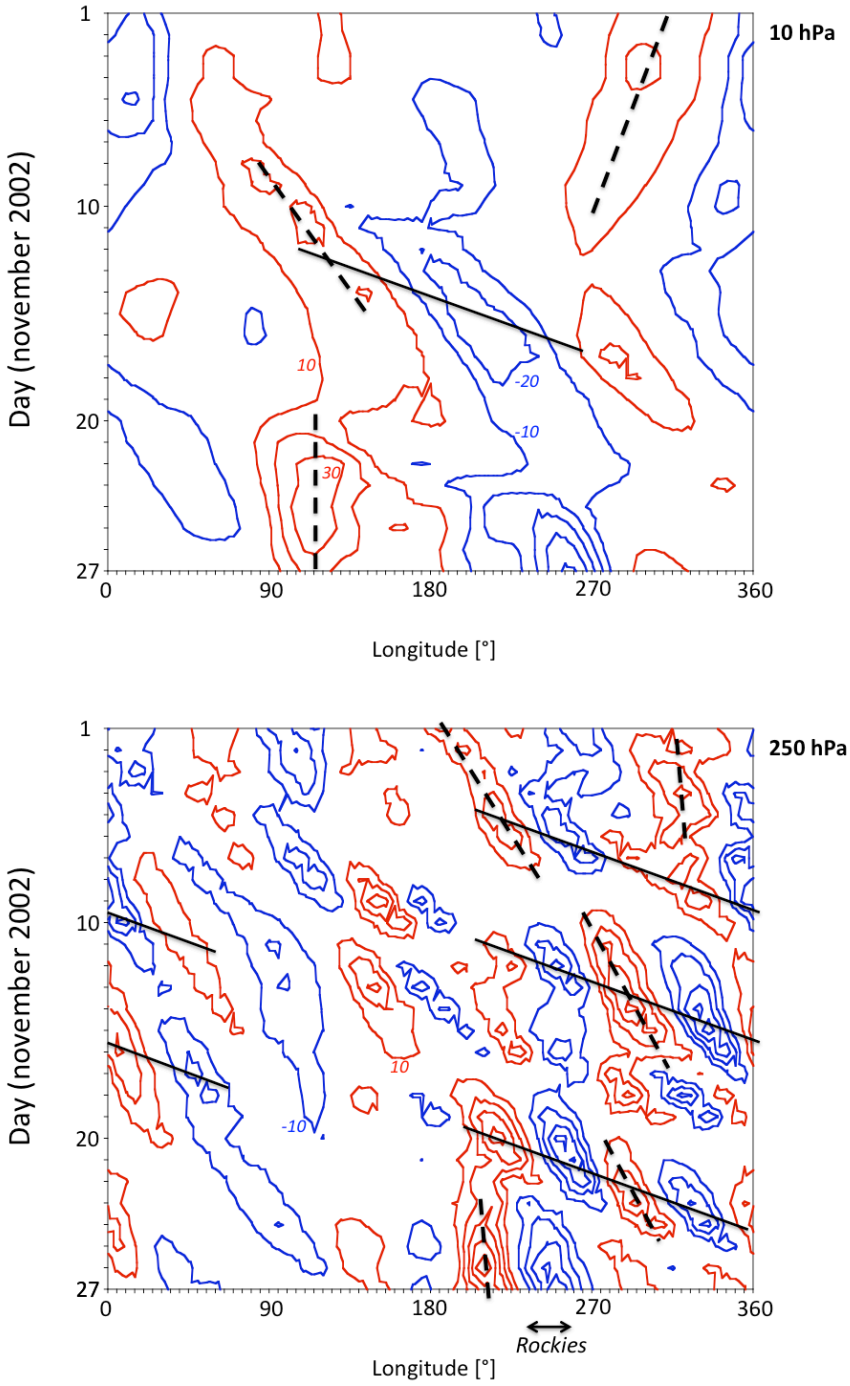

FIGURE 11.1. Time evolution of the meridional component of the velocity, averaged between 40°N and 60°N, as a function of longitude at 10 hPa (upper panel) and at 250 hPa (lower panel) for the period 1-27 November 2002, based on daily mean NCEP-2 reanalysis. The contour interval is 10 m s^{-1}. Red (blue) contours correspond to poleward (equatorward) motion. Slanted solid straight lines indicate a succession of maximum development of meridional flow, characterizing a group of waves. Dashed lines are lines of constant phase. The group speed is nearly 20 m s^{-1}, 3 times the phase speed of the individual troughs and ridges embedded in the group or packet of waves. The most energetic wave activity at 250 hPa is observed in the vicinity and to the east of the Rocky mountains. New waves develop downstream of a wave packet, while mature waves die at the upstream end of the wave packet. This is a characteristic of dispersion (**Box 1.14**). Case taken from the book by Wallace and Hobbs (2006) (see the book list at the end of this chapter). Source of the data: http://www.esrl.noaa.gov/psd/data/gridded/data.ncep.reanalysis2.html.

(see the original Hövmoller diagram in **figure 1.112**). At 250 hPa (about 10 km) (the lower panel of **figure 11.1**) the dominant longitudinal wavelength of the waves is 60 to 70°. At 50°N this is equivalent to a longitudinal wavelength of about 5000 km. In accordance with the linear theory of Rossby-wave propagation (section 1.34) the wave group (indicated by the solid lines) propagates faster in eastward direction than the phase (indicated by the dashed lines). The wave energy (proportional to the air density multiplied by the velocity squared) in the troposphere decreases markedly in the middle and higher stratosphere. At 10 hPa (about 30 km) (the upper panel of **figure 11.1**) wave-activity is not only weaker than in the troposphere, but also of much larger horizontal scale. The dominant waves at 10 hPa have a longitudinal wavelength of more than 10000 km. The relatively short waves do not seem to penetrate into the stratosphere. This is why the Polar winter cyclonic stratospheric vortex is relatively axisymmetric. In summer the anticyclonic stratospheric vortex is even more strongly axisymmetric (**figures 7.3** and **7.4**). This suggests that vertical propagation of Rossby waves from the troposphere into the stratosphere is practically prohibited in summer.

The following 2 sections present a theory that explains these observations. This theory, which was developed by Charney and Drazin[1], is based on the quasi-geostrophic potential vorticity equation. **Section 11.2** is devoted to deriving the quasi-geostrophic potential vorticity equation. **Section 11.3** presents the theory of vertical planetary wave propagation, demonstrating that wave-propagation is influenced very strongly by the zonal mean state. The reverse influence, i.e. the influence of eddies and waves on the zonal mean state, is the subject of the remaining sections in this chapter. We'll see that the existence of the **Ferrel cell** is principally due to the reduction of the zonal mean temperature gradient by the meridional eddy heat flux. The final sections of this chapter are concerned with a theory of the **Brewer-Dobson circulation** (**figure 10.22**). This theory, which envisions the three-dimensional transport of tracers, such as water vapour and ozone, as being the result of a *two-dimensional circulation* in the meridional-vertical plane, leads to some very interesting and simple insights into the interaction between dynamics and diabatics (radiation), the details of which are the subject of **chapter 12**.

11.2 Quasi-geostrophic potential vorticity equation

The quasi-geostrophic vorticity (1.251) and thermodynamic equations (1.316) (with J=0) can be expressed as follows.

$$\frac{\partial \nabla_h^2 \Phi}{\partial t} = -\vec{v}_g \cdot \vec{\nabla}\left(\nabla^2 \Phi\right) + f_0^2 \frac{\partial \omega}{\partial p} - \beta \frac{\partial \Phi}{\partial x} \quad , \tag{11.1a}$$

$$\frac{\partial}{\partial t}\frac{\partial \Phi}{\partial p} = -\vec{v}_g \cdot \vec{\nabla}\frac{\partial \Phi}{\partial p} - \sigma\omega \quad , \tag{11.1b}$$

where, repeating eq. 1.317, the static stability parameters,

$$\boxed{\sigma \equiv \frac{R}{c_p} S_p \text{ and } S_p \equiv \frac{\alpha}{c_p} - \frac{\partial T}{\partial p}} . \tag{11.2}$$

[1] Charney, J.G. and P. Drazin, 1961: Propagation of planetary scale disturbances from the lower atmosphere into the upper atmosphere. **J.Geophys.Res., 66**, 83-109.

(Beware!: *in this chapter σ is not isentropic density*). Defining

$$\chi \equiv \frac{\partial \Phi}{\partial t}, \tag{11.3}$$

we express (11.1a) as (remember: $f=f_0+\beta y$ and $f_0 v_g=\partial \Phi/\partial x$)

$$\frac{1}{f_0}\nabla^2\chi = -\vec{v}_g\cdot\vec{\nabla}\left(\frac{1}{f_0}\nabla^2\Phi + f\right) + f_0\frac{\partial \omega}{\partial p}, \tag{11.4}$$

Now, multiplying (11.1b) by f_0^2/σ and using (11.3) we obtain

$$\frac{f_0^2 p}{RS_p}\frac{\partial \chi}{\partial p} = -\frac{f_0^2 p}{RS_p}\vec{v}_g\cdot\vec{\nabla}\frac{\partial \Phi}{\partial p} - f_0^2\omega.$$

Differentiating this equation with respect to p, and combining the result with (11.4) in order to eliminate ω, we obtain

$$\boxed{\nabla^2\chi + \frac{\partial}{\partial p}\left(\frac{f_0^2}{\sigma}\frac{\partial \chi}{\partial p}\right) = -f_0\vec{v}_g\cdot\vec{\nabla}\left(\frac{1}{f_0}\nabla^2\Phi + f\right) + \frac{\partial}{\partial p}\left[-\frac{f_0^2}{\sigma}\vec{v}_g\cdot\vec{\nabla}\frac{\partial \Phi}{\partial p}\right]}. \tag{11.5}$$

This is the **geopotential tendency equation**. Half-way the twentieth century the geopotential tendency equation was an important equation of dynamical meteorology. It was used to diagnose and understand development of cyclones and anticyclones in mid-latitudes. The geopotential tendency equation is an elliptic partial differential equation, similar in structure to the omega equation (9.31). The left hand side is roughly proportional to $-\chi$ (see the reasoning below eq. 9.31). The right hand side (r.h.s.) of (11.5) represents the "forcing" of the geopotential tendency. The first and second term on the r.h.s. of (11.5) are referred to, respectively, as "advection of vorticity" and "differential temperature advection". The second term on the right hand side of (11.5) can be expressed as

$$\frac{\partial}{\partial p}\left[-\frac{f_0^2}{\sigma}\vec{v}_g\cdot\vec{\nabla}\frac{\partial \Phi}{\partial p}\right] = -\vec{v}_g\cdot\vec{\nabla}\frac{\partial}{\partial p}\left(\frac{f_0^2}{\sigma}\frac{\partial \Phi}{\partial p}\right) - \frac{f_0^2}{\sigma}\frac{\partial \vec{v}_g}{\partial p}\cdot\vec{\nabla}\frac{\partial \Phi}{\partial p}.$$

The second term on the r.h.s. of this equation is equal to zero because the thermal wind,

$$\frac{\partial \vec{v}_g}{\partial p} \propto \vec{v}_T$$

is parallel to the isotherms (section 1.35), while

$$\vec{\nabla}\frac{\partial \Phi}{\partial p} \propto \vec{\nabla}T\ ,$$

obviously, is perpendicular to the isotherms. Therefore, the geopotential tendency equation becomes

$$\frac{1}{f_0}\nabla^2\chi+\frac{\partial}{\partial p}\left(\frac{f_0}{\sigma}\frac{\partial\chi}{\partial p}\right)=-\vec{v}_g\cdot\vec{\nabla}\left(\frac{1}{f_0}\nabla^2\Phi+f\right)-\vec{v}_g\cdot\vec{\nabla}\left(\frac{\partial}{\partial p}\frac{f_0^2}{\sigma}\frac{\partial\Phi}{\partial p}\right). \tag{11.6}$$

With (11.3) this can also be written as

$$\boxed{\left(\frac{\partial}{\partial t}+\vec{v}_g\cdot\vec{\nabla}\right)\left(\frac{1}{f_0}\nabla^2\Phi+f+\frac{\partial}{\partial p}\left(\frac{f_0}{\sigma}\frac{\partial\Phi}{\partial p}\right)\right)\equiv\frac{\mathrm{d}_g q}{\mathrm{d}t}=0}, \tag{11.7}$$

where

$$\boxed{q\equiv\frac{1}{f_0}\nabla^2\Phi+f+\frac{\partial}{\partial p}\left(\frac{f_0}{\sigma}\frac{\partial\Phi}{\partial p}\right)}. \tag{11.8}$$

Eq. 11.6 is the **quasi-geostrophic potential vorticity equation** and q is known as the **quasi-geostrophic potential vorticity**. The first term on the r.h.s. of the definition of q (eq. 11.8) represents the relative vorticity, the second term represents the planetary vorticity and the last term represents the effect of static stability on the quasi-geostrophic potential vorticity. The units of q are [s^{-1}]!

Box 11.1 A model based on quasi-geostrophic potential vorticity inversion

Equation 11.7 is a very powerful equation for describing the adiabatic dynamical evolution of the atmosphere. Assuming, for mathematical simplicity, that σ is constant, a dynamical model of the atmosphere can be based on the following four equations.

$$q\equiv\frac{1}{f_0}\frac{\partial^2\Phi}{\partial x^2}+\frac{1}{f_0}\frac{\partial^2\Phi}{\partial y^2}+f_0+\beta y+\frac{f_0}{\sigma}\frac{\partial^2\Phi}{\partial p^2}; \tag{1}$$

$$\frac{\partial q}{\partial t}=-u_g\frac{\partial q}{\partial x}-v_g\frac{\partial q}{\partial y}\ ; \tag{2}$$

$$u_g\approx-\frac{1}{f_0}\frac{\partial\Phi}{\partial y};\ v_g\approx\frac{1}{f_0}\frac{\partial\Phi}{\partial x}\ . \tag{3}$$

With knowledge of the three-dimensional distribution of the geopotential at a specified time, we can compute the three-dimensional distribution of q using eq. 1. We then proceed to integrate eq. 2 forward in time. At each time step we determine the geostrophic winds by first "inverting" eq. 1 to find Φ from q and then using eq. 3 to determine the velocities. Solving eq. 1 to find Φ from q is referred to as "**quasi-geostrophic potential vorticity-inversion**".

11.3 Vertical propagation of Rossby waves

We assume the presence of a constant time-independent zonal flow, U, which is perturbed slightly. We first introduce a streamfunction, defined as

$$u_g \equiv -\frac{\partial \psi}{\partial y};\ v_g \equiv \frac{\partial \psi}{\partial x}\ ,$$

so that $\psi = \Phi/f_0$. This is consistent with the quasi-geostrophic wind equations (9.16). The streamfunction associated with the perturbed zonal flow can be expressed as

$$\psi = -Uy + \psi'. \tag{11.9}$$

Here ψ' represents the perturbation to the zonal mean time-independent state. The quasi-geostrophic potential vorticity equation, linearised around the time-independent state is

$$\frac{\mathrm{d}_g q}{\mathrm{d}t} \equiv \left(\frac{\partial}{\partial t} + U\frac{\partial}{\partial x}\right)q' + \beta\frac{\partial \psi'}{\partial x} = 0. \tag{11.10}$$

Here $q = Q + q'$, with $Q = f = f_0 + \beta y$ and

$$q' \equiv \nabla^2\psi' + \frac{\partial}{\partial p}\left(\frac{f_0^2}{\sigma}\frac{\partial \psi'}{\partial p}\right). \tag{11.11}$$

If we substitute a solution of the form

$$\psi' = \Psi(p)\exp\left[\mathrm{i}(kx + ly - \omega t)\right] \tag{11.12}$$

into (11.10), we obtain

$$\frac{\partial}{\partial p}\left(\frac{f_0^2}{\sigma}\frac{\partial \Psi}{\partial p}\right) - (k^2 + l^2)\Psi + \frac{\beta k}{(kU - \omega)}\Psi = 0. \tag{11.13}$$

If we can, for simplicity, regard the factor f_0^2/σ as a constant, then eq. 11.13 has the same structure as e.g. eq. 3.23:

$$\frac{f_0^2}{\sigma}\frac{\partial^2 \Psi}{\partial p^2} + m^2\Psi = 0, \tag{11.14}$$

with the **index of refraction** or **wave transmission** coefficient, m, defined by

$$\boxed{m^2 \equiv \frac{\beta k}{(kU - \omega)} - (k^2 + l^2)}, \tag{11.15}$$

Vertically propagating waves with vertical wave number m exist if $m^2 > 0$. On the other hand, if $m^2 < 0$, the wave-amplitude decays with increasing height (see the reasoning below eq.

3.26). The parameter m^2 determines the transmission of waves in the vertical direction.

The value of the index of refraction, m^2, is determined by only two parameters that have nothing to do with the properties of the wave itself. These are β and U. Since the first parameter depends only on y, vertical variations of the index of refraction are determined by vertical variations of the zonal mean zonal wind velocity, U. For instance, if the index of refraction goes from positive to negative at some altitude, a wave will be attenuated if it propagates from the region with postive m^2 to the region with negative m^2. The wave may also be reflected or absorbed. Absorption occurs if m^2 goes to infinity. This is the case if the denominator of the first term on the r.h.s. of (11.15) approaches zero, i.e. if

$$U - c_x = 0, \tag{11.16}$$

Here, $c_x=\omega/k$ is the x-component of the phase speed. The level where (11.16) is satisfied is called the **critical level**.

If we restrict our attention to **stationary waves**, we may put $c_x=0$ (or $\omega=0$). The implication of (11.15) is that stationary Rossby waves penetrate into upper atmosphere if the total horizontal wave number is smaller than $\sqrt{\beta/U}$. Therefore, only relatively long stationary Rossby waves will be observed in the stratosphere (**figure 11.1**). The consequence of this is also that **the mean zonal wind should be eastward for vertical penetration**. Therefore, because in the summer hemisphere the polar stratosphere is dominated by easterlies, i.e there is an anticyclone over the pole, **stationary Rossby waves are observed in the stratosphere only in the winter hemisphere**.

The criterion for vertical propagation of stationary waves, $m^2>0$, can be written as

$$\boxed{0 < U < \frac{\beta}{k^2 + l^2} \equiv U_c}, \tag{11.17}$$

where U_c is called the **Rossby critical velocity**.

For **non-stationary waves** the criterion for vertical propagation without loss of energy (11.15) can be expressed as

$$0 < U - c_x < U_c \ . \tag{11.18}$$

This again underlines the fact that the vertical transmissivity of the atmosphere to planetary waves is very sensitive to the zonal velocity.

Vertical propagation of waves can only occur if the winds are eastward and weaker than a critical strength. The very strong stratospheric winter polar vortex of the southern hemisphere (lower panel of **figure 7.1**) will more likely block and reflect wave activity than the weaker stratospheric winter polar vortex of the northern hemisphere (upper panel of **figure 7.1**). This idea is supported by **figure 11.2**, which shows the climate, for the years 1989 to 2008, of the zonal mean eddy heat flux, $[v^*T^*]$ (defined in section 1.39) at 100 hPa, area averaged between 40°lat and 80°lat, for the northern hemisphere and for the southern hemisphere. The eddy heat flux is frequently used as a measure of the wave forcing from the troposphere to the stratosphere (this will be explained in section 11.7). In **figure 11.2** we observe that this wave forcing undergoes different seasonal cycles in both hemispheres, with a maximum in mid-winter in the northern hemisphere and a maximum in spring in the southern hemisphere. In view of the theoretical ideas, presented above, the relatively weak wave forcing in the southern hemisphere winter would seem to relate to the very intense polar vortex.

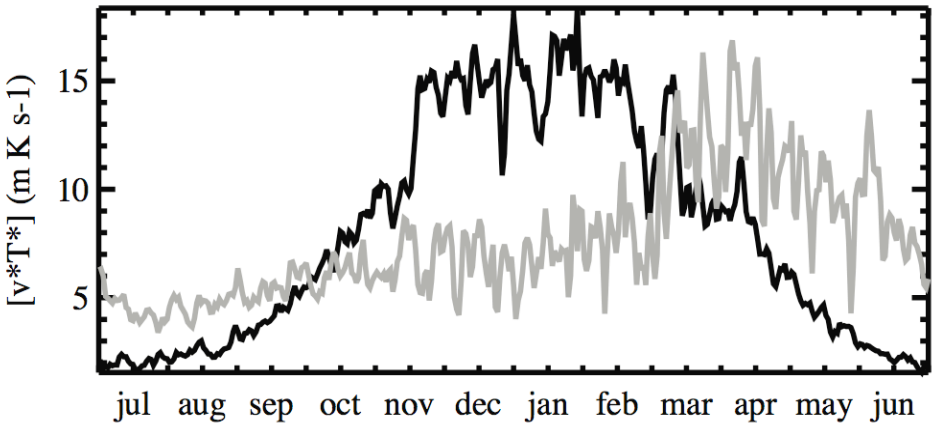

FIGURE 11.2. Daily climate of the poleward eddy heat flux, [v^*T^*], at 100 hPa (area weighted averaged between 40°lat and 80°lat) for the northern hemisphere (black) and for the southern hemisphere, derived from 20 years (1989-2008) of 6-hourly instantaneous values of [v^*T^*], using ERA-Interim reanalysis data. Months indicated along the *x*-axis are for the northern hemisphere. The corresponding months in the southern are shifted by 6 months, i.e. December and March correspond, respectively, to June and September in the southern hemisphere. The sudden increase of the eddy heat flux and associated wave activity in the southern hemisphere in September is hypothesized to be due to the reduction of the average westerly wind velocity in the mid-latitudes in the lower stratosphere after approximately beginning of September (**figure 7.2**). Figure due to Yvonne Hinssen.

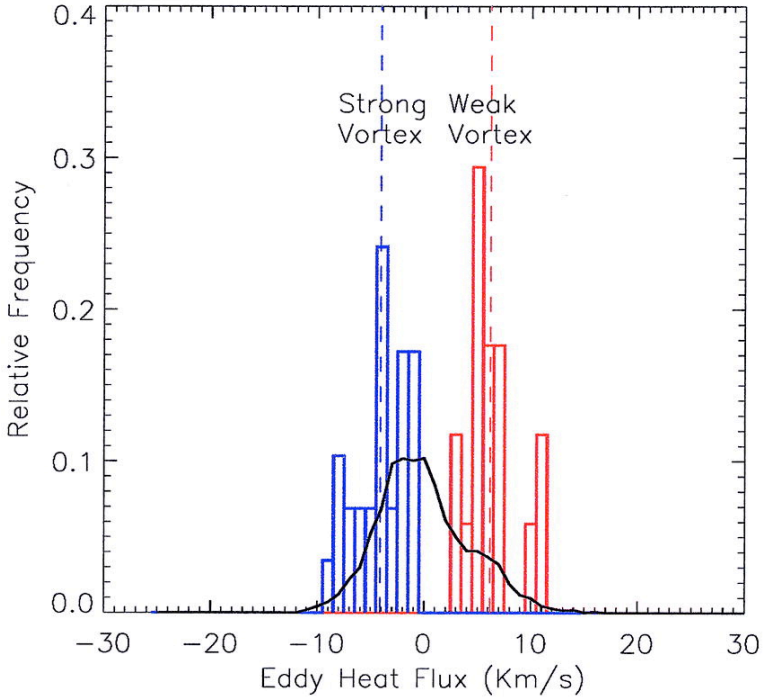

FIGURE 11.3. Probability distributions for the 40-day averaged heat flux *anomaly* at 100 hPa, between 45°N and 75°N, for all winter days (black curve), and the 18 weak vortex (red) and 30 strong vortex (blue) events, as defined in Baldwin and Dunkerton (2001)[2]. Figure from Polvani, L. M., D. W. Waugh, 2004: Upward Wave Activity Flux as a Precursor to Extreme Stratospheric Events and Subsequent Anomalous Surface Weather Regimes. **J. Climate, 17**, 3548–3554.

[2] Baldwin, M. P., and T. J. Dunkerton, 2001: Stratospheric harbingers of anomalous weather regimes. **Science, 294,** 581–584

The relation between the strength of the vortex and wave forcing at 100 hPa is supported by **figure 11.3**, which shows probability distributions for the 40-day averaged eddy heat flux anomaly at 100 hPa between 45°N and 75°N for all winter days from 1958 to 2001 (black curve), for 18 weak vortex events (red) and for 30 strong vortex events (blue). Strong vortex events are clearly associated with lower than normal wave activity in the lower stratosphere, while weak vortex events are associated with stronger than average wave activity in the lower stratosphere. Of course, this does not necessarily indicate that vertical propagation is hindered when the vortex is strong. The direction of the causal link could very plausibly be the other way around, which would imply that the polar vortex is weak (strong) due to enhanced (reduced) mixing of potential vorticity associated with enhanced (reduced) planetary wave activity.

11.4 Zonal average flux equation

Here we derive an equation for zonally averaged meridional flux of momentum and heat, which discriminates between the effect of eddies and the effect of the mean meridional circulation. We start with the following equation for the material time rate of a quantity Q, where S is a source or sink of Q:

$$\frac{dQ}{dt} = S. \tag{11.19}$$

In pressure coordinates this equation is,

$$\frac{\partial Q}{\partial t} + u\left(\frac{\partial Q}{\partial x}\right)_p + v\left(\frac{\partial Q}{\partial y}\right)_p + \omega\frac{\partial Q}{\partial p} = S, \tag{11.20}$$

where

$$\omega \equiv \frac{dp}{dt}. \tag{11.21}$$

The quantity Q may represent the potential temperature, in which case S represents diabatic heating or cooling.

The **mass conservation equation in pressure coordinates** is, neglecting earth's curvature (**section 1.24**),

$$\left(\frac{\partial u}{\partial x}\right)_p + \left(\frac{\partial v}{\partial y}\right)_p + \frac{\partial \omega}{\partial p} = 0\ . \tag{11.22}$$

Multiplying this equation by Q and combining the result with eq. 11.20, yields the **flux-form** of equation (11.20), also called the **continuity equation of *Q***:

$$\frac{\partial Q}{\partial t} + \left(\frac{\partial uQ}{\partial x}\right)_p + \left(\frac{\partial vQ}{\partial y}\right)_p + \frac{\partial \omega Q}{\partial p} = S. \tag{11.23}$$

We now take the zonal average of this equation. Let us use the notation of section 1.39, where square brackets are introduced to indicate a zonal average, while a star is introduced to indicate a deviation from the zonal average. The zonal average of eq. 11.23 is

$$\frac{\partial[Q]}{\partial t}+\frac{\partial[vQ]}{\partial y}+\frac{\partial[\omega Q]}{\partial p}=[S]. \tag{11.24}$$

The zonal average of the meridional flux of a quantity Q is

$$[vQ]=\left[([v]+v^*)([Q]+Q^*)\right]=[v][Q]+[v^*Q^*]. \tag{11.25}$$

Therefore, the zonal average flux divergence equation becomes

$$\frac{\partial[Q]}{\partial t}+\frac{\partial[v][Q]}{\partial y}+\frac{\partial[v^*Q^*]}{\partial y}+\frac{\partial[\omega][Q]}{\partial p}+\frac{\partial[\omega^*Q^*]}{\partial p}=[S]. \tag{11.26}$$

The zonally averaged continuity equation is:

$$\frac{\partial[v]}{\partial y}+\frac{\partial[\omega]}{\partial p}=0. \tag{11.27}$$

Using this, we can write the **flux equation** as

$$\boxed{\frac{\partial[Q]}{\partial t}+[v]\frac{\partial[Q]}{\partial y}+[\omega]\frac{\partial[Q]}{\partial p}+\frac{\partial[v^*Q^*]}{\partial y}+\frac{\partial[\omega^*Q^*]}{\partial p}=[S]}. \tag{11.28}$$

In the following section we'll use this equation as a basis for the derivation of an equation describing the zonal mean meridional circulation (**figure 10.20**). The quantity $[v^*Q^*]$ represents the **zonal mean meridional eddy flux** of Q.

11.5 Zonal mean meridional circulation in midlatitudes (the Ferrel cell)

Let us "apply" eq. 11.28 to the following two equations (see eqs. 12a and 8 of Box 9.1).

$$\frac{du}{dt}=-\frac{\partial\Phi}{\partial x}+fv+F_x; \tag{11.29}$$

$$\frac{dT}{dt}=\frac{RT}{c_p p}\omega+\frac{J}{c_p}. \tag{11.30}$$

The term, F_x, represents a frictional force per unit mass. This gives

$$\frac{\partial[u]}{\partial t}+[v]\frac{\partial[u]}{\partial y}+[\omega]\frac{\partial[u]}{\partial p}+\frac{\partial[v^*u^*]}{\partial y}+\frac{\partial[\omega^*u^*]}{\partial p}=+f[v]+[F_x]; \tag{11.31}$$

$$\frac{\partial[T]}{\partial t}+[v]\frac{\partial[T]}{\partial y}+[\omega]\frac{\partial[T]}{\partial p}+\frac{\partial[v*T*]}{\partial y}+\frac{\partial[\omega*T*]}{\partial p}=+\frac{\kappa}{p}\left([\omega][T]+[\omega*T*]\right)+\frac{[J]}{c_p}. \qquad (11.32)$$

We now make the following approximation:

$$\frac{\partial[\omega*u*]}{\partial p}<<\frac{\partial[v*u*]}{\partial y} \text{ and } \frac{\partial[\omega*T*]}{\partial p}<<\frac{\partial[v*T*]}{\partial y}; \qquad (11.33)$$

This must be supported by evidence from observations, reanalysis data or numerical simulations. An inspection of the magnitude of the four different terms in (11.33) during the evolution of the simulated life cycle of an unstable baroclinic wave, which is described in section 10.7, reveals the general validity of the inequalities in (11.33). Furthermore:

$$[v]=[v_g]+[v_a]=\left[\frac{1}{f}\frac{\partial\Phi}{\partial x}\right]+[v_a]=[v_a]; \qquad (11.34)$$

With (11.33) and (11.34) the zonal mean *x*-momentum equation, (11.31), becomes

$$\frac{\partial[u]}{\partial t}=-[v_a]\frac{\partial[u]}{\partial y}-[\omega]\frac{\partial[u]}{\partial p}+f[v_a]-\frac{\partial[v*u*]}{\partial y}+[F_x], \qquad (11.35)$$

while the temperature equation (11.32) becomes

$$\frac{\partial[T]}{\partial t}=-[v_a]\frac{\partial[T]}{\partial y}-[\omega]\frac{\partial[T]}{\partial p}+\frac{\kappa[T]}{p}[\omega]+\frac{\kappa}{p}[\omega*T*]-\frac{\partial[v*T*]}{\partial y}+\frac{[J]}{c_p}. \qquad (11.36)$$

For mathematical simplicity, we further simplify eqs. 11.35 and 11.36 by assuming that

$$[\omega]\frac{\partial[u]}{\partial p}<<[v_a]\frac{\partial[u]}{\partial y}\ ; \qquad (11.37a)$$

$$\frac{\partial[u]}{\partial y}<<f\approx f_0; \qquad (11.37b)$$

$$[v_a]\frac{\partial[T]}{\partial y}<<\left(\frac{\kappa[T]}{p}-\frac{\partial[T]}{\partial p}\right)[\omega]\equiv S_p[\omega], \qquad (11.37c)$$

and

$$-[\omega]\frac{\partial[T]}{\partial p}+\frac{\kappa[T]}{p}[\omega]+\frac{\kappa}{p}[\omega*T*]\equiv S_p[\omega]+\frac{\kappa}{p}[\omega*T*]\approx S_p[\omega]\ ;$$

in which we thus require that

$$\frac{\kappa}{p}[\omega*T*]<<S_p[\omega], \qquad (11.37d)$$

The static stability is defined as

$$\boxed{S_p \equiv \left(\frac{\kappa [T]}{p} - \frac{\partial [T]}{\partial p} \right) = -\frac{[T]}{[\theta]} \frac{\partial [\theta]}{\partial p} > 0}, \tag{11.38}$$

In the troposphere, the zonal mean static stability, $S_p \approx 5 \times 10^{-4}$ K Pa^{-1}.

Assumption (11.37a) is definitively not valid in general. Furthermore, assumption (11.37b) is in fact equivalent to stating that the Rossby number (section 1.23) is much smaller than 1, which is not a very robust assumption either. Nevertheless, it is thought that the physical content of the equations is not seriously affected by the application of these assumptions. Assumptions (11.37c) and (11.37d), on the other hand, are quite robust, at least in the quite realistic baroclinic life-cycle simulation, which is described in section 10.7.

By applying (11.37a,b,c,d), eqs. 11.35 and 11.36 simplify to

$$\boxed{\frac{\partial [u]}{\partial t} = f_0 [v_a] - \frac{\partial [v^* u^*]}{\partial y} + [F_x]}; \tag{11.39a}$$

$$\boxed{\frac{\partial [T]}{\partial t} = S_p [\omega] - \frac{\partial [v^* T^*]}{\partial y} + \frac{[J]}{c_p}}. \tag{11.39b}$$

We assume that the zonal mean state conforms to hydrostatic balance and gesotrophic balance as follows (Box 9.1):

$$\frac{\partial [\Phi]}{\partial p} = -\frac{R[T]}{p}; \tag{11.40a}$$

$$f_0 [u] = -\frac{\partial [\Phi]}{\partial y}. \tag{11.40b}$$

From these two equations we derive an equation for thermal wind balance of the zonal mean state:

$$f_0 \frac{\partial [u]}{\partial p} = \frac{R}{p} \frac{\partial [T]}{\partial y}. \tag{11.41}$$

Consistent with the continuity equation (11.27) we may introduce a streamfunction, ψ, with units [Pa m s^{-1}] as follows.

$$\boxed{[v_a] \equiv \frac{\partial \psi}{\partial p}; [\omega] \equiv -\frac{\partial \psi}{\partial y}}. \tag{11.42}$$

Taking the time derivative of the equation for zonal mean thermal wind balance (11.41) we may write,

$$f_0 \frac{\partial}{\partial p} \frac{\partial [u]}{\partial t} = \frac{R}{p} \frac{\partial}{\partial y} \frac{\partial [T]}{\partial t}, \tag{11.43}$$

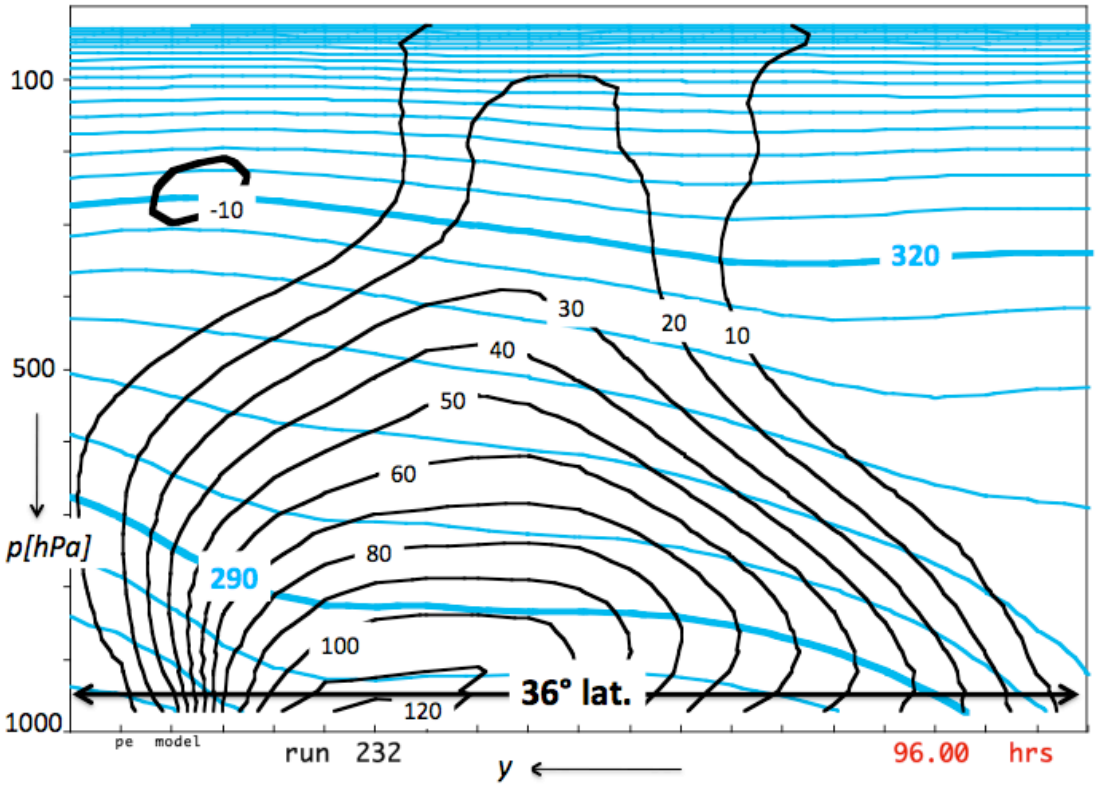

FIGURE 11.4. Meridional cross-section showing the zonal average meridional eddy temperature flux, $[v^*T^*]$ (solid black contours, labeled in units of K m s^{-1}], and zonal average potential temperature (**cyan**, labeled in units of K) at t=4 days in the simulation of an unstable baroclinic wave, described in chapter 10. The initial state is shown in **figure 10.6**.

Which, upon substitution of (11.39a,b), yields

$$\frac{\partial^2\psi}{\partial y^2}+\frac{f_0^2 p}{S_p R}\frac{\partial^2\psi}{\partial p^2}=\frac{f_0 p}{S_p R}\frac{\partial^2[v^*u^*]}{\partial p\partial y}-\frac{1}{S_p}\frac{\partial^2[v^*T^*]}{\partial y^2}-\frac{f_0 p}{S_p R}\frac{\partial[F_x]}{\partial p}+\frac{1}{c_p S_p}\frac{\partial[J]}{\partial y}, \qquad (11.44)$$

Eq. 11.44, which is referred to as the "**Kuo-Eliassen equation**"[3], describes the zonal mean meridional circulation in mid-latitudes that is required to maintain thermal wind balance in the presence of processes that disturb this state of balance. We shall refer to this meridional circulation as the "**zonal mean ageostrophic response**", which is a short way of saying that it represents the **response required to maintain zonal mean thermal wind balance**. The processes that disturb *zonal mean* thermal wind balance are eddy fluxes of momentum (first term on the r.h.s. of eq. 11.26), eddy fluxes of sensible heat (second term on the r.h.s. of eq. 11.26), the zonal average zonal frictional force (third term on the r.h.s. of eq. 11.26) and diabatic heating or cooling (fourth term on the r.h.s. of eq. 11.26). The Kuo-Eliassen equation is an elliptic partial differential equation (Box 7.1), similar to the potential vorticity inversion (7.12) (see also eq. 1 of **Box 11.1**), the Sawyer-Eliassen equation (8.32) and the

[3] Kuo, H-L., 1956: Forced and free meridional circulations in the atmosphere. **J.Atmos.Sci., 13**, 561-568. Eliassen, A., 1952: Slow thermally or frictionally controlled meridional circulations in a circular vortex. **Astrophys.Norv., 5**, 19-60.

omega equation (9.31). If the streamfunction is specified at the boundaries of the domain of solution, the Kuo-Eliassen equation can be solved by the techniques that have been described in chapters 7 and/or 9.

Retaining only the forcing due to the eddy flux of heat in the forcing term on the r.h.s. of (11.44), the Kuo-Eliassen equation reduces to

$$\boxed{\frac{\partial^2\psi}{\partial y^2}+\frac{f_0^2 p}{S_p R}\frac{\partial^2\psi}{\partial p^2}=-\frac{1}{S_p}\frac{\partial^2[v^*T^*]}{\partial y^2}\equiv F}\,. \tag{11.45}$$

The arguments below (9.31) can be applied also here. Therefore,

$$\boxed{\frac{\partial^2\psi}{\partial y^2}+\frac{f_0^2 p}{S_p R}\frac{\partial^2\psi}{\partial p^2}\propto -\psi}\,, \tag{11.46}$$

so that eq. 11.45 becomes (approximately)

$$\boxed{-\psi\propto F}\,. \tag{11.47}$$

There is one dominant maximum in the eddy heat flux, shown in **figure 11.4**. Roughly speaking, this means that the associated forcing term, F, on the r.h.s. of eq. 11.45 is positive everywhere in this domain, which implies that $\psi<0$ everywhere. Assuming **zero zonal mean mass-flow perpendicular to the boundaries**, we may set

$$\psi=0 \tag{11.48}$$

at all boundaries. At the side boundary this is not a realistic condition (**figure 10.20**). A solution to this problem is to position the side boundary of the domain of solution of eq. 11.45 relatively far away from the region of non-zero forcing, i.e. the region with a non-zero eddy heat flux, and still impose the boundary condition (11.48). With the definition of $[\omega]$ in terms of the streamfunction (11.42), we conclude that there must be zonal mean ascent north of the central latitude, $y=y_0$, and zonal mean descent south of the central latitude, which agrees with the direction of the meridional circulation shown in **figure 10.20**. This circulation is illustrated schematically in **figure 11.5**. Positive eddy heat fluxes in middle latitudes are therefore responsible for forcing of an **indirect meridional circulation** (descending warm air and rising cold air), called the "**Ferrel circulation**" (**figures 10.21 and 10.22**).

Let us solve the Kuo-Eliassen equation with only forcing due to meridional eddy heat flux included, i.e. eq. 11.45, for an idealized situation that approximately resembles the situation in the simulation of the life cycle of a baroclinic wave on the f-plane (section 10.7) at t=96 hrs (**figure 11.4**). The eddy heat flux is poleward nearly everywhere. The maximum eddy heat flux is $[v^*T^*]$=120 K m^{-1} and near the Earth's surface at the latitude $y=y_0$ (**figure 11.4**). This can be approximated mathematically as

$$[v^*T^*]=120\cos\left(\frac{\pi(y-y_0)}{2y_{scale}}\right)\cos\left(\frac{\pi(p_s-p)}{2p_{scale}}\right) \text{ if } |y-y_0|\le y_{scale} \text{ and } py_0\le p\le p_s; \tag{11.49a}$$

$$[v^*T^*]=0 \text{ otherwise.} \tag{11.49b}$$

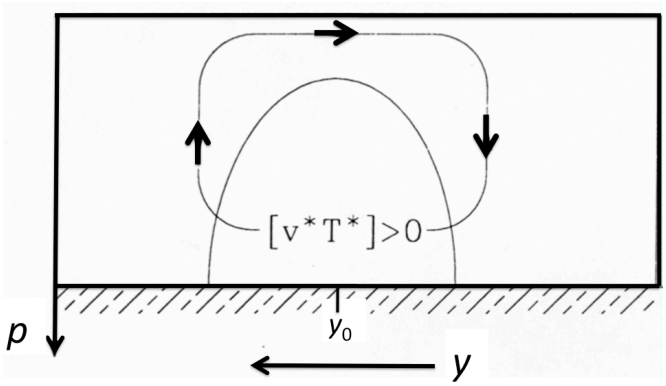

FIGURE 11.5. The meridional circulation induced by positive (poleward) eddy temperature fluxes within the semi-circle. The North Pole is on the left hand side of the figure. The area of positive meridional eddy heat flux is symmetrical about the latitude, $y=y_0$. Adapted from James (1994) (see list of books at the end of this chapter).

Here, y_{scale}=1500 km and p_{scale}=500 hPa represent, respectively, the meridional scale and the vertical scale of the area of zonal mean positive (poleward) heat flux. The forcing term on the r.h.s. of 11.45 is

$$F = -\frac{120}{S_p}\frac{\pi^2}{4\left(y_{scale}\right)^2}\cos\left(\frac{\pi\left(y-y_0\right)}{2y_{scale}}\right)\cos\left(\frac{\pi\left(p_s-p\right)}{2p_{scale}}\right) \text{ if } |y-y_0|\le y_{scale} \text{ and } py_0 \le p \le p_s; \quad (11.50a)$$

$$F = 0 \text{ otherwise.} \quad (11.50b)$$

Eq. 11.45 is solved by the numerical relaxation method that is described in section 9.9 (see also Box 7.2). The two-dimensional domain of solution is divided into equal grid-cells with dimensions Δy and Δp. A grid point is identified by its index (j, k), where j represents the index in the positive y-direction and k represents the index in the positive p-direction. The discrete form of eq. 11.45 is

$$\frac{1}{\Delta y^2}\left(\psi[j+1,k]+\psi[j-1,k]\right)+\frac{f_0^2 p[j,k]}{S_p R\Delta p^2}\left(\psi[j,k+1]+\psi[j,k-1]\right)-2\left(\frac{1}{\Delta y^2}+\frac{f_0^2 p[j,k]}{S_p R\Delta p^2}\right)\psi[j,k]$$
$$-F[j,k]=0, \quad (11.51)$$

where the "forcing" is given eq. 11.50a,b. As a boundary condition we simply set ψ=0 at all boundaries. As an initial guess of the solution we substitute ψ=0 into (11.51). The r.h.s. of eq. 11.51 will then almost certainly yield a non-zero residual. We then use this residual, *RES*, to obtain a better guess of the solution at the grid point (j,k), i.e.

$$\left\{\psi[j,k]\right\}_{new}=\left\{\psi[j,k]\right\}_{old}+\left(\frac{2}{\Delta y^2}+\frac{2f_0^2 p[j,k]}{S_p R\Delta p^2}\right)^{-1} RES, \quad (11.52)$$

in which case the new residual at grid point (j,k) is reduced to zero. However, the residuals at the neighbouring grid points are not yet reduced to zero. Nevertheless, if we repeat this procedure for each grid point in sequence, we will note that the residual at all grid points approaches zero asymptotically for sufficient repetitions of these steps. With an appropriate

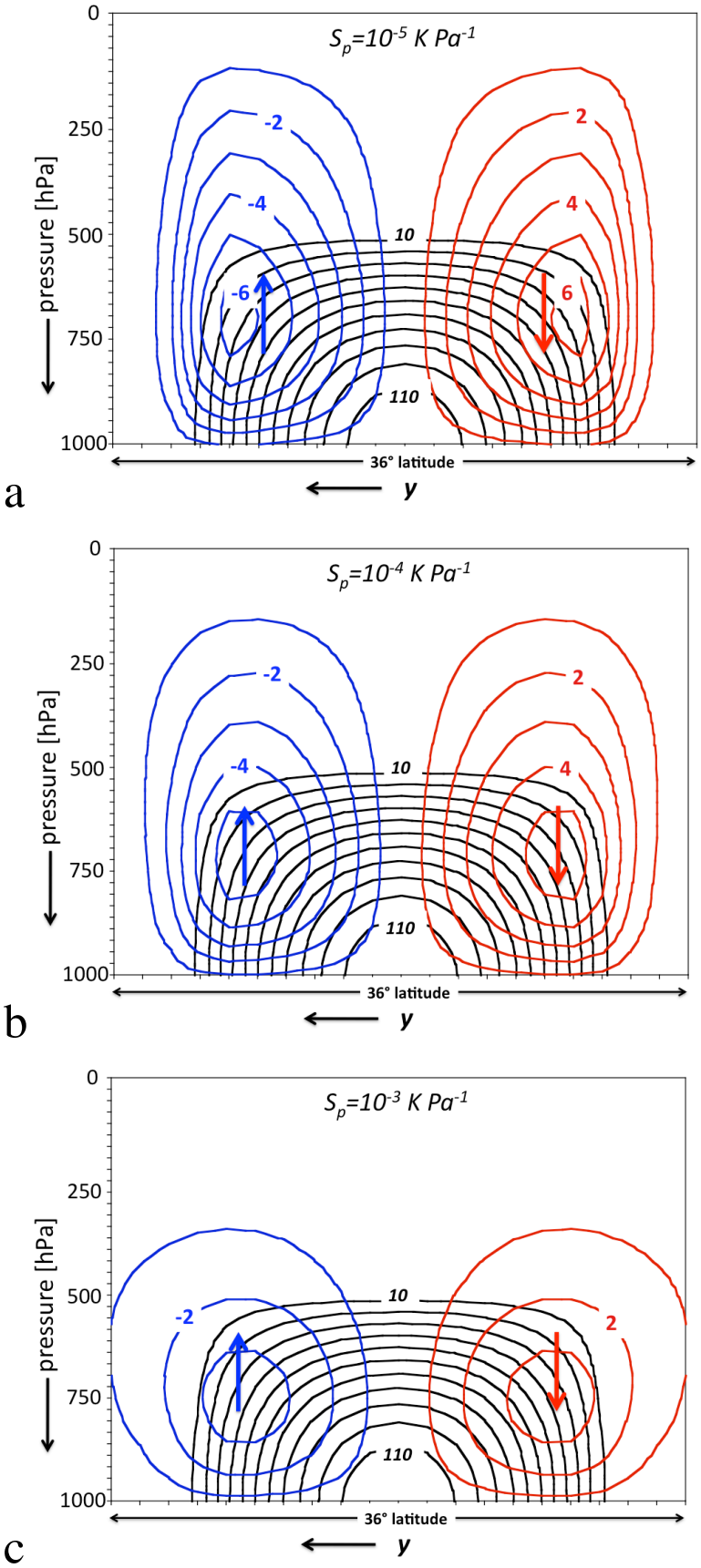

FIGURE 11.6: The solution eq. 11.45, for three values of S_p (f_0=10^{-4} s^{-1}), in terms of the vertical velocity (labeled in units of 0.1 hPa hr^{-1}), with prescribed eddy heat flux (eq. 11.49), shown in black (label in units of K m s^{-1}). **Red** (**blue**) corresponds to **downward** (**upward**) motion.

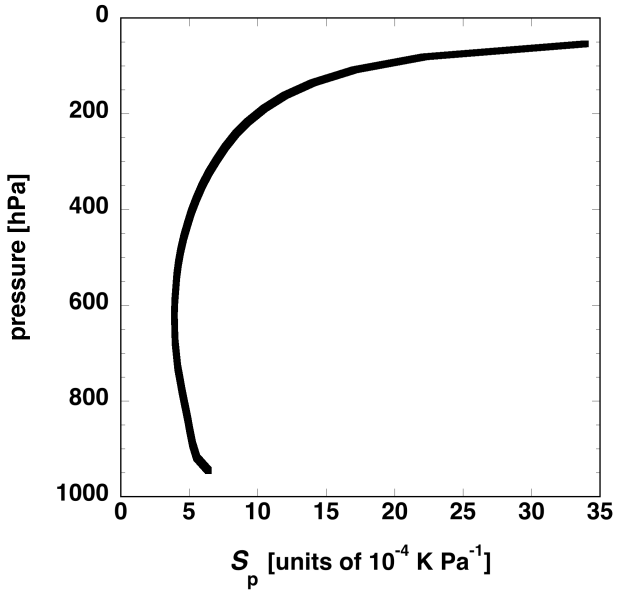

FIGURE 11.7: The *horizontal domain average value* of the static stability as a function of pressure at t=96 hrs in the run described in section 10.7.

convergence criterium we can obtain an acceptable numerical solution of eq. 11.45.

The solution is shown in **figure 11.6** for three cases. The domain of solution spans a latitudinal distance, which is twice as large, i.e. 72°. Only the central part of this domain is shown. The three cases differ only in the prescribed value of the static stability parameter, S_p (eq. 11.38). The values are S_p=10^{-5} K Pa^{-1} (upper panel), 10^{-4} K Pa^{-1} (middle panel) and 10^{-3} K Pa^{-1} (lower panel). In all cases f_0=0.0001 s^{-1}. The *horizontal domain-averaged* (below 400 hPa) value of S_p in the simulation of section 10.7, corresponding to t=96 hours (**figure 11.4**), is 5×10^{-4} K Pa^{-1} (**figure 11.7**). Therefore, case (b) and case (c) are most comparable to the situation shown in **figure 10.20**. According to the solution of the quasi-geostrophic Kuo-Eliassen equation (11.45), eddy heat fluxes force an indirect meridional circulation. The intensity of this circulation is weaker in **figure 11.6** than it is in **figure 10.20.** Nevertheless, the Kuo-Eliassen provides a qualitatively consistent explanation for the existence of the indirect circulation..

Figure 11.6 demonstrates that lower static stability, not only leads to an intensification of the meridional circulation, but also leads to a reduction of the aspect ratio (the horizontal scale divided by the vertical scale) of the meridional circulation. When the atmosphere is very stable (large value of S_p) the meridional circulation is relatively "flat" and weak (lower panel of **figure 11.6**). By analogy of the Kuo-Eliassen equation (11.45) with the two-dimensional omega equation (9.87) and based on the arguments leading form eq. 9.87 to 9.98, we conclude that the aspect ratio of the Ferrel cell is governed by the following equation:

$$\frac{L_y}{\Delta p} = \frac{2\pi}{f_0}\sqrt{\frac{S_p R}{p}} = \frac{2\pi}{f_0}\sqrt{\sigma}\ , \tag{11.53}$$

or, with σ=2×10^{-6} m^{2}Pa^{-1}s^{-1},

$$\Delta p = \frac{f_0}{2\pi\sqrt{\sigma}} L_y \approx 100 L_y\,. \tag{11.54}$$

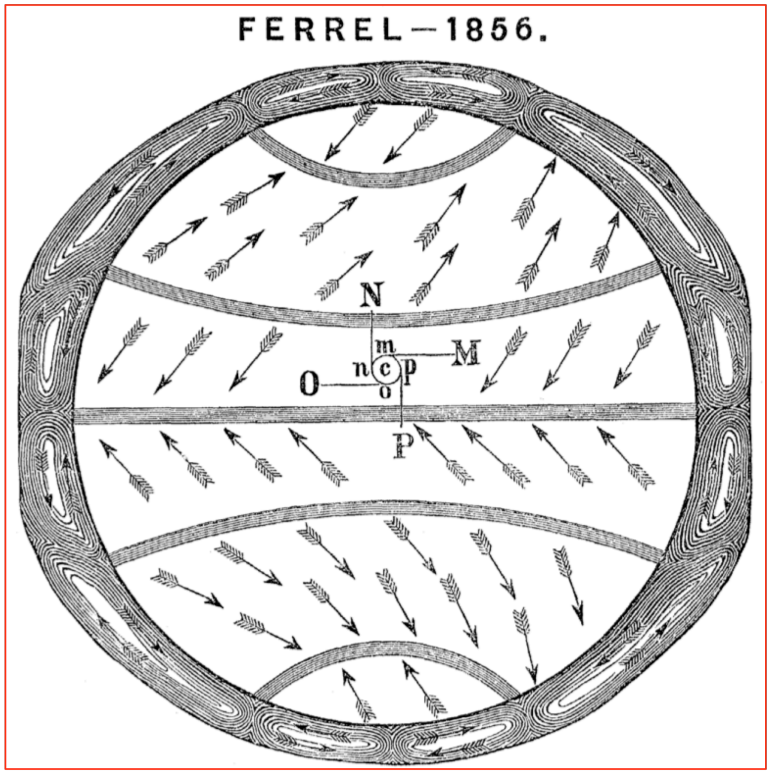

FIGURE 11.8. The annual average wind-vector near the surface of the Earth and the meridional circulations as correctly envisioned by William Ferrel in 1856.

L_y is determined by the meridional width of the "cyclone track", which is approximately equal to the meridional width of the region of positive eddy heat flux (i.e. approximately 3000 km). We thus find that the "upward penetration" of the Ferrel circulation is about 300 hPa, and that this must increase with decreasing static stability, as is indeed found from the solution of eq. 11.45 (**figure 11.6**).

The existence of an indirect meridional circulation implies that the average near surface winds in the northern hemisphere in mid-latitudes blow from the south-west (see **figure 11.8**), while on average the winds veer with increasing height, consistent with warm air advection, i.e. with heat transport from the equator to the pole (section 1.35).

The sensible heat flux by eddies is directed down the gradient of the zonal average temperature, i.e. poleward. This has led many researchers to parametrise the heat flux by eddies in zonally symmetric models of the general circulation as

$$[v^* T^*] = -K_h \frac{\partial [T]}{\partial y}, \tag{11.55}$$

where K_h is a positive **eddy diffusion coefficient** and the derivative with respect to y is performed at constant pressure. This parametrisation is directly related to Prandtl's "mixing length" turbulence theory (**section 1.8**). Unfortunately, an analogous parametrisation does not hold for the eddy flux of eastward momentum (**figure 11.9**). The zonal mean linear momentum per unit mass on the f-plane is (eq. 1.120)

$$[M] = [u] - f_0 y \ . \tag{11.56}$$

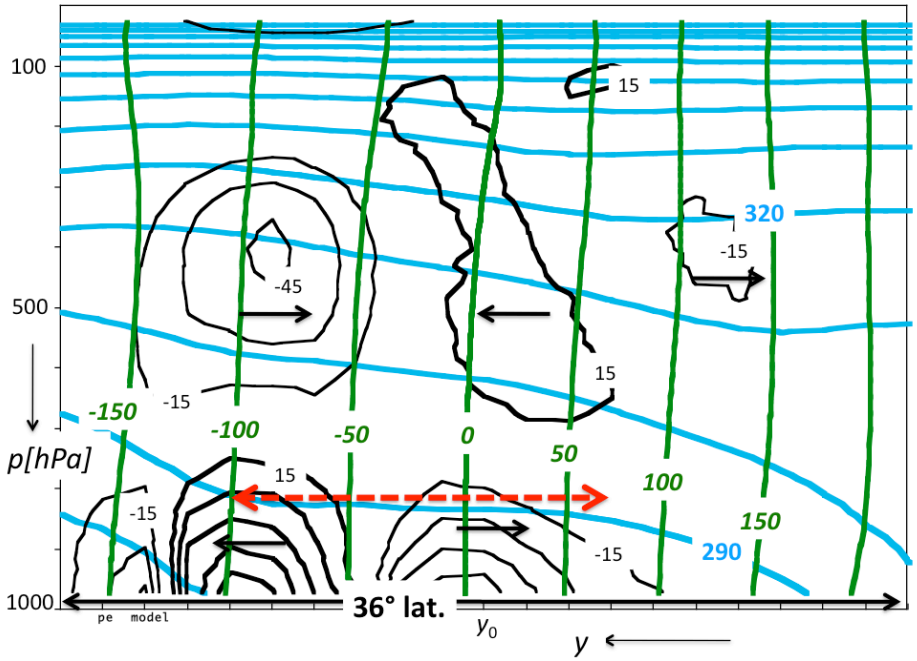

FIGURE 11.9: Meridional cross-section showing the zonal average meridional flux of eastward momentum, $[u^*v^*]$ (solid black contours, labeled in units of $m^2\ s^{-2}$], and the zonal average potential temperature (**cyan**, labeled in units of K) and the zonal average linear momentum per unit mass, $[M]$ (**green**, labeled in $m\ s^{-1}$, assuming y_0=0) at t=4 days in the primitive equation model simulation of an unstable baroclinic wave on an "f-plane" (constant Coriolis parameter, $f_0=10^{-4}\ s^{-1}$), which is described in section 10.7. The arrows indicate the direction of the eddy momentum flux. The double dashed arrow indicates the eddy-mixing zone. The corresponding eddy heat flux is shown in **figure 11.4**. The initial state is shown in **figure 10.5**. Note that eddy-momentum flux in this numerical simulation bears no relation to the *gradient* of zonal mean linear momentum, $\partial[u]/\partial y \approx -f_0$ (see the text). It should also be noted that this instantaneous distribution of momentum flux by eddies is not representative for the whole simulated life-cycle. In other words, the pattern of eddy momentum flux is quite variable in time, in contrast to the pattern of eddy sensible heat flux.

In view of (11.37b), the meridional gradient of $[M]$ is approximately equal to $-f_0$, which is negative on the northern hemisphere. From Prandtl's theory we now expect a poleward flux of eastward momentum due to the action of eddies at all latitudes on the northern hemisphere. However, **figure 11.9** reveals that this is not the case. Apparently, the eddy flux of eastward momentum in the numerical simulation may be directed *up* the gradient of average eastward momentum. The American meteorologist, Victor Starr, has associated this phenomenon with *negative* viscosity[4]. Note (**figure 11.9**) that the eddy momntum fluxes converge in the upper troposphere in the middle of the domain, which implies that eddies accelerate the zonal mean zonal flow.

The indirect Ferrel circulation tranports sensible heat equatorwards, opposite in direction to the eddy flux of sensible heat. But, the meridional heat flux by eddies is always larger than the meridional heat flux by the Ferrel cell, so that the **net heat flux is poleward**. In the zonal mean view of the evolution of an *adiabatic* atmosphere (as is the case in this simulation) this net poleward heat flux is manifested as a downward movement of the isentropes on the poleward cold side of the front and a simultaneous upward movement of

[4] V. P. Starr, 1968: **Physics of Negative Viscosity Phenomena.** MacGraw-Hill, 256 pp.

the isentropes on the equatorward warm side of the front (**figure 11.10**). In an adiabatic atmosphere isentropes are material surfaces. Therefore, **figure 11.10** suggests that air parcels are moving upward on the equatorward side of the front and downward on the poleward side of the front. In other words, the zonal mean "Lagrangian" meridional circulation is direct, whereas the Ferrel circulation (**figure 10.20**), which is the result of a "Eulerian" average of the meridional and vertical velocity, is indirect. The Lagrangian meridional circulation is of physical interest because this circulation reveals the actual direction of the zonal mean meridional mass flux, which is usually dominated by the poleward eddy mass flux. Indeed, in **figure 11.10** we observe an increase of mass between θ=290 K and θ=305 K for $y>y_0$, and a decrease of the mass between θ=290 K and θ=305 K for $y<y_0$. The layer between θ=290 K and θ=305 K belongs to the Middleworld. The opposite is the case in the Underworld, i.e. between the earth's surface and θ=290 K. **We may conclude that in an adiabatic unstable baroclinic wave mass flows poleward in the Middleworld and equatorward in the Underworld**, as is illustrated in **figure 10.22**. The following section derives a set of approximate equations, which provides insight into the driving mechanism of the zonal mean poleward mass flux in and above the Middleworld.

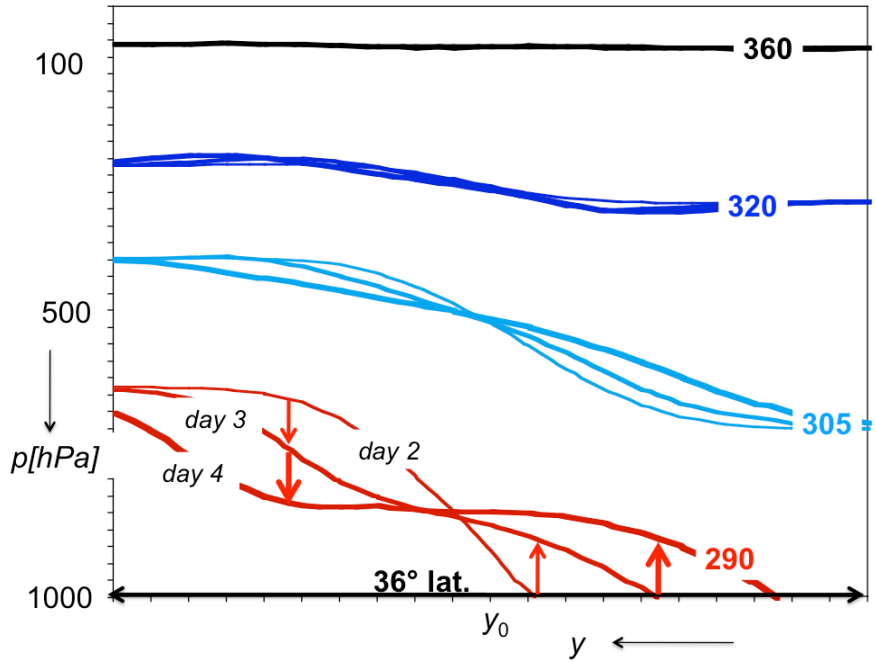

FIGURE 11.10: The zonal mean position of selected isentropes at t=2 days (thin contours), at t=3 days (thicker contours) and at t=4 days (thick contours) during the simulation of the adiabatic life cycle of an unstable baroclinic wave. The initial state is shown in **figure 10.6**. Each arrow indicates the change in vertical position of the 290 K isentrope during 1 day.

PROBLEM 11.1. **Meridional circulation forced by the eddy flux of easward momentum**

(a) Devise an analytical expression, similar to eq. 11.49, that best approximates the distribution of the eddy flux of eastward momentum in **figure 11.9** and solve the Kuo-Eliassen equation with only this forcing effect included: i.e.

$$\frac{\partial^2\psi}{\partial y^2}+\frac{f_0^2 p}{S_p R}\frac{\partial^2\psi}{\partial p^2}=\frac{f_0 p}{S_p R}\frac{\partial^2[v^*u^*]}{\partial p\partial y}. \qquad (11.57)$$

Will the eddy flux of eastward momentum also force an indirect meridional circulation and thus reenforce the indirect circulation that is forced by the eddy heat flux?
(b) Can you add the individual solutions of eqs. 11.45 and 11.57 in order to obtain solution of the full equation:

$$\boxed{\frac{\partial^2\psi}{\partial y^2}+\frac{f_0^2 p}{S_p R}\frac{\partial^2\psi}{\partial p^2}=\frac{f_0 p}{S_p R}\frac{\partial^2[v*u*]}{\partial p\partial y}-\frac{1}{S_p}\frac{\partial^2[v*T*]}{\partial y^2}}\ ? \qquad (11.58)$$

PROBLEM 11.2. **Sensitivity of the Ferrel cell to variations in static stability and Coriolis parameter**
(a) What value of the Coriolis parameter, f_0, will yield a solution of the Kuo-Eliassen equation 11.45 which is identical to that shown in the middle panel of **figure 11.6** if $S_p=10^{-6}$ K Pa^{-1}?
(b) Check whether the aspect ratios of the circulations, shown in **figure 11.6**, are approximately in accord with the eq. 11.54.

PROBLEM 11.3. **Applicability of eddy diffusion theory**
Based on **figures 10.6 and 11.4**, discuss the applicability of the theory of eddy diffusivity (Prandtl's mixing length theory[5]) to the eddy flux of sensible heat in a two-dimensional (zonal mean) model of the general circulation.

11.6 Transformed Eulerian Mean (TEM) and Eliassen-Palm flux

This section discusses an analytical model of the interaction of eddies with the zonal mean state of the atmosphere, which interprets the influence of eddies as a drag force on the zonal mean zonal flow and, furthermore, provides insight into the interaction between adiabatic processes and diabatic processes.

We begin with the "**Eulerian mean**" quasigeostrophic equations, governing the zonal mean zonal wind and zonal mean temperature are (see eqs. 11.39a, 11.39b):

$$\frac{\partial[u]}{\partial t}=f_0[v_a]-\frac{\partial[v*u*]}{\partial y}+[F_x]. \qquad (11.59)$$

and

$$\frac{\partial[T]}{\partial t}=S_p[\omega]-\frac{\partial[v*T*]}{\partial y}+\frac{[J]}{c_p}. \qquad (11.60)$$

Let us introduce the following "**residual velocities**":

$$\boxed{[\omega]_r\equiv[\omega]-\frac{\partial}{\partial y}\frac{[v*T*]}{S_p}} \qquad (11.61)$$

[5] http://en.wikipedia.org/wiki/Mixing_length_model

and

$$\boxed{\left[v_a\right]_r \equiv \left[v_a\right] + \frac{\partial}{\partial p}\frac{\left[v^*T^*\right]}{S_p}} \,. \tag{11.62}$$

The residual velocities, $[v_a]_r$ and $[\omega]_r$, can be interpreted as "physically consistent" velocity components, because they satisfy the following "continuity equation", which is analogous to the "real" continuity equation (11.22):

$$\boxed{\frac{\partial\left[v_a\right]_r}{\partial y} + \frac{\partial\left[\omega\right]_r}{\partial p} = 0} \,. \tag{11.63}$$

The residual velocities represent the "**transformed Eulerian zonal mean velocity components**" of the zonal mean "**residual flow**". A difficult aspect of this "residual flow" is that it does not satisfy the "usual" boundary conditions at the Earth's surface. For example, in the idealized situation of **figure 11.6**, where $[\omega]=0$ at the Earth's surface, the residual flow should be downward at the Earth's surface (i.e. $[\omega]_r>0$) poleward of the region of maximum eddy heat flux and upward at the Earth's surface (i.e. $[\omega]_r<0$) equatorward of the region of maximum eddy heat flux. In view of these pecularities, the theory to be described in the following is usually not applied only to the "Underworld" (**figure 1.48**). The lower boundary of the Middleworld is usually taken to be the 300 K or 310 K isentrope. The lower boundary of the Overworld is usually taken to be the 370 K or 380 K isentrope.

Substituting (11.61) and (11.62) into (11.59) and (11.60) yields the following **transformed Eulerian mean** (**TEM**) equations, which govern the time rate of change of the zonal mean zonal wind and zonal mean temperature:

$$\boxed{\frac{\partial\left[u\right]}{\partial t} = f_0\left[v_a\right]_r - \frac{\partial\left[u^*v^*\right]}{\partial y} - f_0\frac{\partial}{\partial p}\frac{\left[v^*T^*\right]}{S_p} + \left[F_x\right]} \tag{11.64}$$

and

$$\boxed{\frac{\partial\left[T\right]}{\partial t} = S_p\left[\omega\right]_r + \frac{\left[J\right]}{c_p}} \,. \tag{11.65}$$

The effects of eddies are manifested in only one of the two equations, i.e. in eq. 11.64. The temperature equation (11.65) is remarkably simple. Averaged over sufficiently long time this equation reveals that **adiabatic heating** (first term on the r.h.s. of eq. 11.65) is balanced by **diabatic heating** (second term on the r.h.s. of eq. 11.65), or cross-isentropic flow. Note that such a stationary state will not occur in the numerical simulation of the *adiabatic* life cycle of an unstable baroclinic wave, which is described at length in section 10.7.

Eq. 11.64 can be written in short as (assuming, for simplicity, that $F_x=0$)

$$\boxed{\frac{\partial\left[u\right]}{\partial t} = f_0\left[v_a\right]_r + \vec{\nabla}\cdot\vec{F}}, \tag{11.66}$$

where

$$\vec{\nabla} \equiv \left(0, \frac{\partial}{\partial y}, \frac{\partial}{\partial p}\right), \tag{11.67}$$

and where

$$\boxed{\vec{F} \equiv \left(-[u^* v^*], -\frac{f_0}{S_p}[v^* T^*]\right)}. \tag{11.68}$$

is called the **"Eliassen-Palm (EP) flux vector"** [6]. It is easily concluded from eq. 11.66 that the **zonal mean zonal flow is accelerated in regions where the EP-flux vector diverges and decelerated in regions where the EP- flux vector converges**. The EP-flux vector is a crucial quantity in understanding the effect of eddies and waves on the zonal average state of the atmosphere. In the "TEM-view" of the general circulation the eddies act to transfer momentum between regions of "eddy- or wave-generation" and regions of "eddy- or wave-dissipation". In the following few sections we will further elaborate upon the implications of this simple[7] and attractive view of eddy-zonal mean flow interaction, which became popular very quickly after its first publication at the end of the 1970's.

11.7 Stationary diabatic- or the wave drive circulation

The TEM-thermodynamic equation (11.65) states that, in a **stationary state**, the adiabatic temperature tendency, due to the vertical component of the residual mean flow, is in balance with the diabatic temperature tendency, due to heating or cooling by e.g. radiation, i.e.

$$\boxed{[\omega]_r = -\frac{[J]}{S_p c_p} \approx -\frac{[\Pi]}{S_p c_p}\left[\frac{d\theta}{dt}\right]} \tag{11.69}$$

In other words, under stationary conditions, or averaging over long periods of time (longer than the time scale of the life-cycle of a baroclinic wave), the **vertical component of the residual flow can be identified with the cross-isentropic flow**, $d\theta/dt$ (section 7.3), i.e. the vertical velocity in the isentropic coordinate system. This is why the residual circulation is frequently referred to as the "**diabatic circulation**", but some prefer to call it the "**wave-driven circulation**"[8].

Figure 11.11 shows the zonal mean, monthly mean "**diabatic residual vertical motion**" in March and June up to θ=500 K (about 50 hPa), according to the ERA40-reanalysis for the period 1979 to 2002. Upwelling is observed in the tropics, approximately between 30°S and 30°N, and downwelling elsewhere, even in the summer hemisphere! This pattern of diabatic heating or cross-isentropic flow, which is not expected on the grounds of only radiation theory (see e.g. **figure 2.24** and section 12.3), is a direct consequence of eddy heat and momentum transport. This can easily be distilled from eq. 11.66, which contains the full effect of eddies on the zonal mean state of the atmosphere.

---

[6] Eliassen, A. and E. Palm, 1960: On the transfer of energy in stationary mountain waves. **Geofys. Publ., 22**, , no.3, p1-23.

[7] Somewhat over-simplified, as is indicated in **box 12.1**.

[8] Shepherd, T.G, 2002: Issues in stratosphere-troposphere coupling. **J.Meteorol.Soc.Japan, 80**, 769-792.

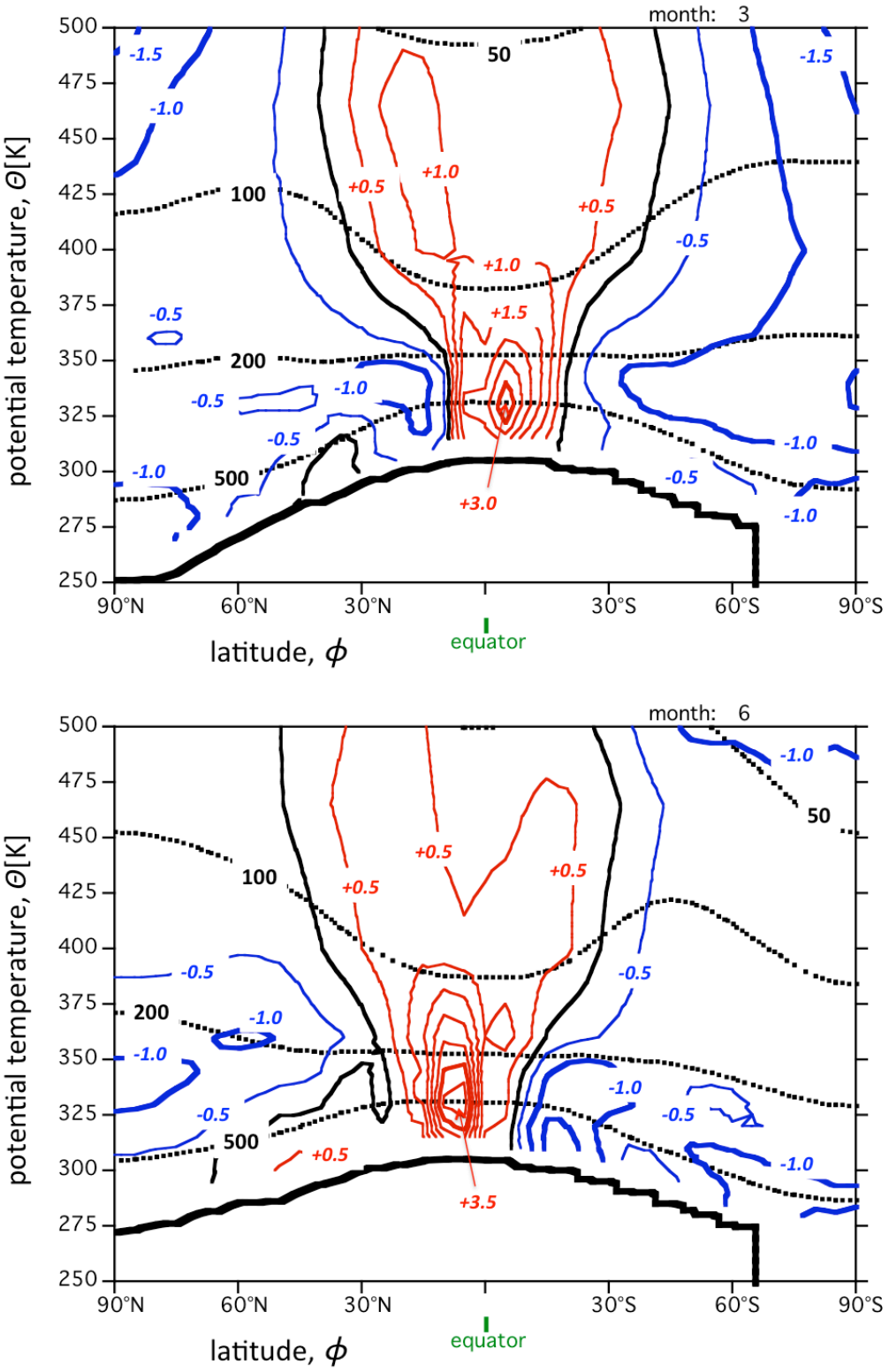

FIGURE 11.11. Zonal mean monthly mean isobars (dashed black lines, labelled in units of hPa) and monthly mean tendency of the *potential* temperature (cross-isentropic flow) (labelled in units of K day^{-1}; contour interval is 0.5 K day^{-1}) as a function of latitude and potential temperature for March (upper panel) and for June (lower panel) according to the ERA-40 reanalysis. The thick black line indicates the zonal mean, monthly mean position of the Earth' surface. The average is for the period 1979-2002. Contours are not drawn if pressure is greater than 750 hPa. Data provided by Paul Berrisford and Yvonne Hinssen.

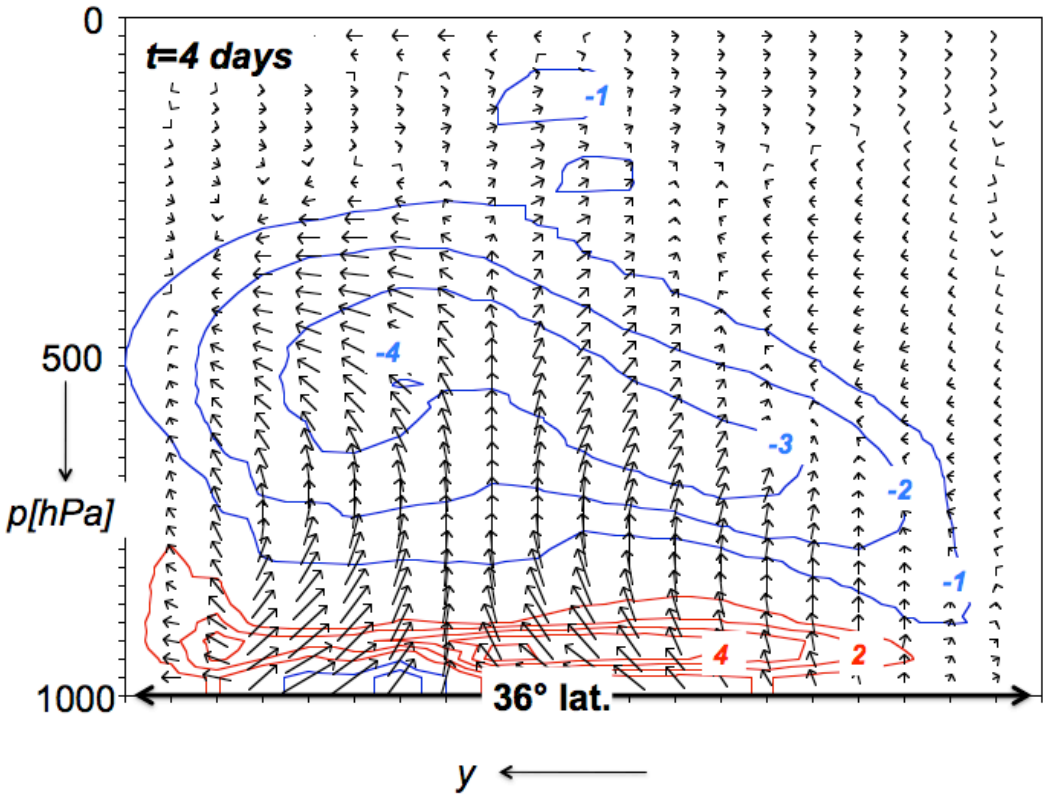

FIGURE 11.12. Instantaneous Eliassen-Palm flux vector and its divergence at *t*=4 days in the primitive equation model simulation of a growing baroclinic wave on an *f*-plane, which is discussed in detail in section 10.7. The horizontal component of the EP-flux vector is magnified 12 times compared to the vertical component. The contours of EP-flux divergence are labeled in units of 10^{-2} m s^{-2}.

The notion that divergence or convergence of zonal momentum due to the eddy meridional momentum flux should reduce or enhance the zonal velocity is intuitively logical. This effect of eddies (and waves) is referred to as "**eddy-stress**" or "**wave-drag**" in sections 1.8 and 3.5. Here we see that the meridional heat flux, due to the action of planetary waves and eddies, has an identical effect on the zonal flow. We shall see in chapter 12 that it is difficult to exagerate the crucial effect of "planetary wave-drag", in regions of EP-flux vector convergence, on the zonal mean state of the upper troposphere and stratosphere.

Equally important for understanding the atmospheric general circulation is the fact that the zonal mean zonal flow is accelerated in regions of EP-flux vector divergence. This effect explains the **existence of the mid-latitude surface westerlies** (**figure 10.19**). It also explains the existence of so-called **eddy-driven jets**, which arrise in the upper troposphere due to eddy mixing of potential vorticity, which weakens the meridional gradient of potential vorticity in the mixing zone and at the same time enhances this gradient at the northern and southern edges of this mixing zone (**chapter 7**). Qualitatively in accord with the solution of the PV-inversion equation, eddy-driven jets are observed at the edges of the mixing zone.

Figure 11.12 shows the instantaneous EP-flux vectors and their divergence at *t*=4 days in the baroclinic life cycle simulation, which is presented in section 10.7 (**figures 11.4** and **11.8**). The EP-flux vector is upward nearly everywhere, which is always the case if the wave transports heat poleward. In the upper half of the region of strongest baroclinic wave growth the EP-flux vector divergence is in general negative. In a stationary state this would lead to

$$\left[v_a\right]_r = -\frac{1}{f_0}\vec{\nabla}\cdot\vec{F} > 0 \ , \qquad (11.70)$$

This implies a poleward residual flow in mid-latitudes. Due to continuity (eq. 11.63) and the asymmetric upper and lower boundary conditions on this residual flow (see section 11.8), the residual flow is upward on the tropical side and downward on the poleward side of the baroclinic wave. This effect of planetary wave drag in the stratosphere on the zonal mean state of the troposphere is referred to as "**Downward Control**" [9]. In the tropics air is drawn upwards from the troposphere through the tropical tropopause into the stratosphere. The term "**extra-tropical pump**" is used to describe the effect of wave-drag in mid-latitudes on the **upwelling in the tropics**. This forced tropical upwelling is thought to be the cause of the very low temperatures that are observed in the upper tropical troposphere (**figure 1.2**). The very cold layer of air, coinciding with the tropical tropopause, is referred to as a "**cold trap**" because air passing through this layer is "**freeze-dried**". If true, this would explain the very low relative humidity of the lower stratosphere.

The *time-average* effect of unstable baroclinic waves on the zonal mean state of the atmosphere (the general circulation) can, thus, be associated with a drag force on the zonal mean zonal flow in the upper troposphere and lower stratosphere, which is equivalent, on average, to a deceleration in the order of 10^{-4} m s^{-2} (about 10 m s^{-1} day^{-1})[10]. In mid-latitudes this is comparable in magnitude to the acceleration due to a Coriolis force, which is exerted on an air parcel that is travelling with a velocity of 1 m s^{-1}, i.e. implying that $[v_a]_r \approx 1$ m s^{-1}. Since zonal velocities in stratosphere are usually much larger, the drag force usually does not strongly disturb the state of geostrophic balance or thermal wind balance. Nevertheless, if this wave drag is sustained for long periods of time (months to years), it does lead to a systematic drift of air (in particular of ozone) from the tropics towards the poles. In the following section we evaluate this drift from the solution of an alternative form of the Kuo-Eliassen equation.

11.8 Residual mean meridional circulation

As explained in **section 11.7**, planetary wave drag, in particular in the mid-latitude upper troposphere and stratosphere, leads to a poleward drift of air and, due to continuity, downwelling over the poles and upwelling in the tropics. This meridional flow is referred to as the **Brewer-Dobson "circulation"**. The term "circulation" is placed in between inverted commas because we have thus far exclusively used this term to indicate the poleward drift of air in the upper troposphere and stratosphere. It is not clear whether the equatorward return flow occurs in the lower troposphere or in the upper stratosphere or mesosphere, although there are strong indications that the return occurs in the Underworld (**figures 10.22 and 11.10**).

Based on eq. 11.63 we may introduce a **residual streamfunction**, χ, so that

$$\left[v_a\right]_r \equiv \frac{\partial\chi}{\partial p}; \left[\omega\right]_r \equiv -\frac{\partial\chi}{\partial y} \ . \qquad (11.71)$$

---

[9] Haynes, P.H. et al., 1991: On the "Downward Control" of extratropical diabatic circulations by eddy-induced mean zonal forces.**J.Atmos.Sci., 48,** 651-678.

[10] Instantaneous deceleration can be much larger, such as at day 4 of the simulated baroclinic life cycle of section 10.7

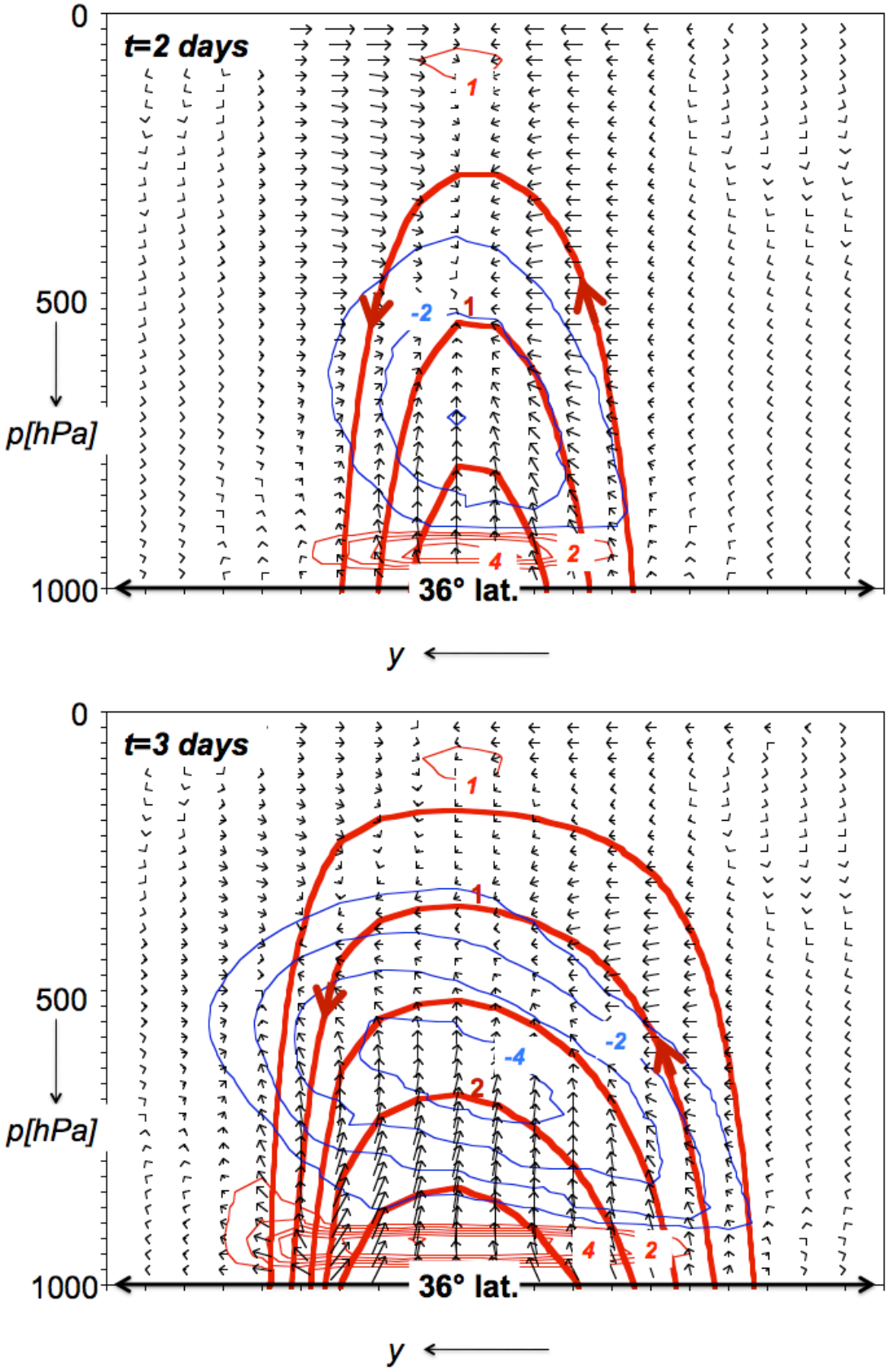

FIGURE 11.13. Continued on next page. For caption see next page.

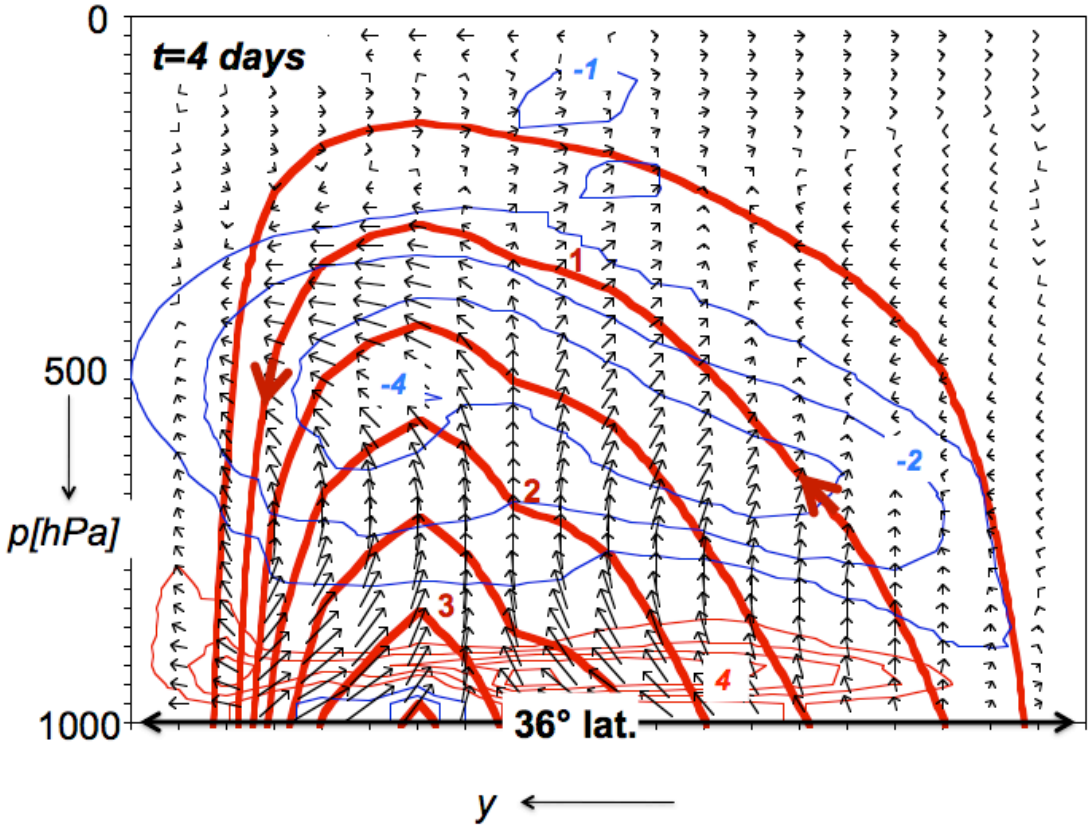

FIGURE 11.13. EP-flux vectors (black arrows), EP-flux divergence (thin solid blue (negative) and red (positive) contours) and residual circulation streamfunction, χ, (thick solid red contours) at three instances in time (after 2 days, after 3 days and after 4 days of simulation) during the baroclinic life-cycle simulation on an *f*-plane, described in section 10.7. The horizontal component of the EP-flux vector is magnified 12 times compared to the vertical component. The contours of EP-flux divergence are labeled in units of 10^{-2} m s^{-2}. The contours of χ are labeled in units of 10^{6} m^{2} s^{-1}. The residual circulation seems to cross the Earth's surface. If this flow is downward, this may be interpreted as a manifestation of an increase in pressure at the earth's surface.

Assuming thermal wind balance (eq. 11.43,), we can easily derive, from (11.65) and (11.66), the following equation for the residual mean meridional circulation:

$$\boxed{\frac{\partial^2 \chi}{\partial y^2} + \frac{f_0^2 p}{R S_p}\frac{\partial^2 \chi}{\partial p^2} = -\frac{f_0 p}{R S_p}\frac{\partial}{\partial p}\left(\vec{\nabla}\cdot\vec{F}\right) + \frac{1}{c_p S_p}\frac{\partial [J]}{\partial y}} \,. \tag{11.72}$$

This equation represents the **transformed Eulerian mean Kuo-Eliassen equation**. At the Earth's surface $[\omega] \approx 0$ so that

$$[\omega]_r \equiv -\frac{\partial \chi}{\partial y} \approx -\frac{\partial}{\partial y}\frac{[v^* T^*]}{S_p} \,, \tag{11.73}$$

which implies that at the Earth's surface we should impose

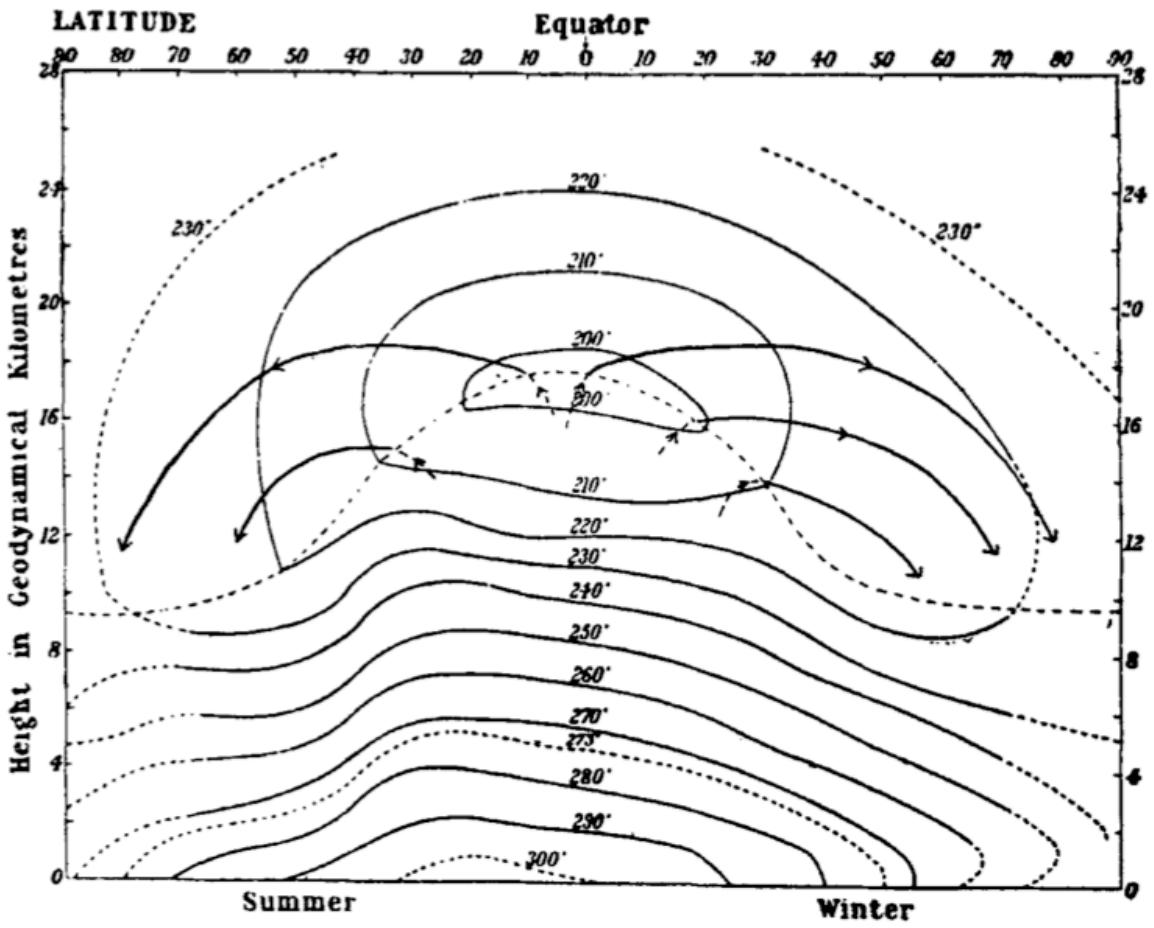

FIGURE 11.14. Brewer's (1949) original figure, illustrating what came to be known as the Brewer-Dobson circulation. "A supply of dry air is maintained by a slow mean circulation from the equatorial tropopause". The contours represent isotherms, labeled in units of K. The **cold point tropopause** corresponds to the equatorial region at about 17 km above the earth's surface where the temperature dips below 200 K.

$$\chi \approx \frac{[v^* T^*]}{S_p} \tag{11.74}$$

Let us assume that

$$\chi = 0 \tag{11.75}$$

at the side- and top-boundaries of the domain of solution of eq. 11.72. Furthermore, in the simulation of chapter 10 we assume $[J]=0$, i.e. we have **adiabatic conditions**. Note that vertical motion in adiabatic conditions implies vertical motion of isentropes. We proceed to solve eq. 11.72 for the distribution of the EP-flux divergence from the output of the model run of section 10.7. The results for day 2, 3 and 4 are shown **figure 11.13**. As expected, **the residual mean circulation is direct**, i.e. there is downwelling on the poleward cold side and upwelling on the equatorward warm side of the baroclinic wave. The residual flow is poleward at levels where the EP-flux converges. Therefore, in the two-dimensional (zonal mean) picture of the general circulation, the effect of zonal asymmetries (waves and eddies) appears as a motion of isentropes towards higher pressure on the cold poleward side of the

baroclinic wave, resulting in downward bulging isentropes, and a motion of the isentropes towards lower pressure on the warm equatorward side of the baroclinic wave, resulting in upward bulging isentropes over the tropics. This can be observed **figure 11.10**.

This explains the existence of the **cold point tropopause** (**figure 11.14**). However, in the real *non-adiabatic* atmosphere polar adiabatic downwelling or tropical adiabatic upwelling, forced by the heat and momentum flux by eddies (i.e "planetary wave drag"), will drive the temperature above or below the radiatively determined temperature (eq. 11.65), which will enhance radiative cooling or heating, and drive the atmosphere towards a stationary state in which diabatic cooling or heating counteracts adiabatic heating or cooling at poleward or equatorward latitudes (**figure 11.11**). The residual circulation is then forced by *both* planetary wave drag *and* diabatic heating/cooling. The interpretation of $[v_a]_r$ and $[\omega]_r$ as the horizontal and vertical components of the projection onto the zonal mean state of the atmosphere of a lagrangian circulation that transports tracers poleward or equatorward is then well founded. This is the stratospheric circulation that Alan Brewer proposed in his attempt to explain the low water vapour content of the stratosphere (**figure 11.14**). His explanation was as follows:

"The observed distributions can be explained by the existence of a circulation in which air enters the stratosphere at the equator, where it is dried by condensation, travels in the stratosphere to temperate and polar regions, and sinks into the troposphere. The sinking, however, will warm the air unless it is being cooled by radiation and the idea of a stratosphere in radiative equilibrium must be abandoned. The cooling rate must lie between about 0.1 and 1.1 °C per day but a value near 0.5°C per day seems most probabale. At the equator the ascending air must be subject to heating by radiation.

The circulation is quite reasonable on energy considerations. It is consistent with the existence of lower temperatures in the equatorial stratosphere than in the polar and temperate regions, and if the flow can carry ozone from the equator to the poles then it gives a reasonable explanation of the high ozone values observed at high latitudes. The dynamical consequences of the circulation are not considered. It should be noted that there is considerable difficulty to account for the smallness of the westerly winds in the stratosphere, as the rotation of the earth should convert the slow poleward movement into strong westerly winds".[11]

The last point, which was raised by Brewer, kept him and his colleagues busy for about 3 decades after 1949. This resulted in the quasi-geostrophic residual circulation theory, which is explained in this and the previous sections (the "TEM"-theory). The "smallness of the westerly winds" is explained in this theory by introduction of the concept of "wave-drag". The complex nonlinear interaction between dynamics and diabatic heating (radiative as well as latent) is the fascinating topic of the following chapter.

11.9 Planetary wave drag and the eddy flux of potential vorticity

One of the attractive features of the TEM-equations (11.64-65) is that the eddy term occurs explicitly only in the momentum equation (11.64) in the form of the EP-flux divergence. However, the physical interpretation of this term as a manifestation of "planetary wave drag" is rather unsatisfactory. It is easy to understand that eddy momentum flux divergence can be associated with a force that acts on the zonal mean flow. However, it is difficult to

[11] Brewer, A.W., 1949: Evidence for a world circulation provided by the measurements of helium and water vapour distribution in the stratosphere. **Q.J.R.Meteorol.Soc., 75**, 351-363.

imagine exactly how eddy sensible heat fluxes could have an identical effect. In this section it is shown that EP-flux divergence can be associated with an eddy flux divergence of zonal mean potential vorticity (PV). From PV inversion (chapter 7) we can understand the consequences of rearrangements of zonal mean PV on the zonal mean balanced zonal flow. The demonstration is given for the quasi-geostrophic case.

We start by repeating the quasi-geostrophic PV-equation (11.7):

$$\frac{d_g q}{dt} = \frac{\partial q}{\partial t} + u_g \frac{\partial q}{\partial x} + v_g \frac{\partial q}{\partial y} = 0 \ . \tag{11.76}$$

Taking the zonal mean of this equation (section 11.4) yields

$$\frac{\partial [q]}{\partial t} + \frac{\partial [v^* q^*]}{\partial y} = 0 \ . \tag{11.77}$$

(the zonal average of the meridional component of the geostrophic velocity is equal to zero; see eq. 11.34). In eq. 11.77 $[q]$ is the zonal average quasi-geostrophic potential vorticity:

$$[q] \equiv \frac{1}{f_0} \frac{\partial^2 [\Phi]}{\partial y^2} + f_0 + \beta y + \frac{\partial}{\partial p}\left(\frac{f_0}{\sigma} \frac{\partial [\Phi]}{\partial p} \right) \tag{11.78}$$

And q^* is the departure from the zonal average quasi-geostrophic potential vorticity:

$$q^* \equiv \frac{1}{f_0}\left(\frac{\partial^2 \Phi^*}{\partial x^2} + \frac{\partial^2 \Phi^*}{\partial y^2} \right) + \frac{\partial}{\partial p}\left(\frac{f_0}{\sigma} \frac{\partial \Phi^*}{\partial p} \right) . \tag{11.79}$$

The eddy potential vorticity flux is

$$[v^* q^*] = \left[\frac{v^*}{f_0}\left(\frac{\partial^2 \Phi^*}{\partial y^2} + \frac{\partial^2 \Phi^*}{\partial y^2} \right) \right] + \left[v^* \frac{\partial}{\partial p}\left(\frac{f_0}{\sigma} \frac{\partial \Phi^*}{\partial p} \right) \right] . \tag{11.80}$$

Assuming that

$$f_0 v^* = \frac{\partial \Phi^*}{\partial x} \text{ and } f_0 u^* = -\frac{\partial \Phi^*}{\partial y} \ , \tag{11.81}$$

we arrive at (see **Box 11.2**)

$$[v^* q^*] = -\frac{\partial}{\partial y}[u^* v^*] + \frac{\partial}{\partial p}\left[f_0 v^* \left(\frac{1}{\sigma} \frac{\partial \Phi^*}{\partial p} \right) \right] . \tag{11.82}$$

Since (eq. 11.2 and eq. 1 of **Box 9.1**)

$$\sigma = \frac{R}{p} S_p \text{ and } \frac{\partial \Phi^*}{\partial p} = -\frac{RT^*}{p}$$

Box 11.2. Derivation of eq. 11.82

The eddy-potential vorticity flux is

$$\left[v^* q^*\right] = \left[\frac{v^*}{f_0}\left(\frac{\partial^2 \Phi^*}{\partial x^2} + \frac{\partial^2 \Phi^*}{\partial y^2}\right)\right] + \left[v^* \frac{\partial}{\partial p}\left(\frac{f_0}{\sigma}\frac{\partial \Phi^*}{\partial p}\right)\right]. \tag{1}$$

Assuming that

$$f_0 v^* = \frac{\partial \Phi^*}{\partial x}\ , \tag{2}$$

this becomes

$$\left[v^* q^*\right] = \left[\frac{1}{f_0^2}\frac{\partial \Phi^*}{\partial x}\left(\frac{\partial^2 \Phi^*}{\partial x^2} + \frac{\partial^2 \Phi^*}{\partial y^2}\right)\right] + \left[\frac{\partial \Phi^*}{\partial x}\frac{\partial}{\partial p}\left(\frac{1}{\sigma}\frac{\partial \Phi^*}{\partial p}\right)\right], \tag{3}$$

which becomes

$$\left[v^* q^*\right] = \frac{1}{f_0^2}\left[\frac{\partial \Phi^*}{\partial x}\frac{\partial^2 \Phi^*}{\partial x^2}\right] + \frac{1}{f_0^2}\left[\frac{\partial \Phi^*}{\partial x}\frac{\partial^2 \Phi^*}{\partial y^2}\right] + \left[\frac{\partial \Phi^*}{\partial x}\frac{\partial}{\partial p}\left(\frac{1}{\sigma}\frac{\partial \Phi^*}{\partial p}\right)\right], \tag{4}$$

or

$$\left[v^* q^*\right] = \frac{1}{f_0^2}\left[\frac{1}{2}\frac{\partial}{\partial x}\left(\frac{\partial \Phi^*}{\partial x}\right)^2\right] + \frac{1}{f_0^2}\left[\frac{\partial \Phi^*}{\partial x}\frac{\partial^2 \Phi^*}{\partial y^2}\right] + \left[\frac{\partial \Phi^*}{\partial x}\frac{\partial}{\partial p}\left(\frac{1}{\sigma}\frac{\partial \Phi^*}{\partial p}\right)\right]. \tag{5}$$

The first term on the r.h.s. of this equation is zero, while the second term becomes

$$\frac{1}{f_0^2}\left[\frac{\partial \Phi^*}{\partial x}\frac{\partial^2 \Phi^*}{\partial y^2}\right] = \frac{1}{f_0^2}\left(\left[\frac{\partial}{\partial y}\left(\frac{\partial \Phi^*}{\partial x}\frac{\partial \Phi^*}{\partial y}\right)\right] - \frac{1}{2}\left[\frac{\partial}{\partial x}\left(\frac{\partial \Phi^*}{\partial y}\right)^2\right]\right) = -\left(\frac{\partial}{\partial y}\left[v^* u^*\right]\right), \tag{6}$$

with (see eq. 11.81)

$$f_0 u^* = -\frac{\partial \Phi^*}{\partial y} \quad \text{and} \quad f_0 v^* = \frac{\partial \Phi^*}{\partial x}\ . \tag{7}$$

Thus,

$$\left[v^* q^*\right] = -\frac{\partial}{\partial y}\left[v^* u^*\right] + \left[\frac{\partial \Phi^*}{\partial x}\frac{\partial}{\partial p}\left(\frac{1}{\sigma}\frac{\partial \Phi^*}{\partial p}\right)\right], \tag{8}$$

or, employing the same trick as in eq. 6,

$$\left[v^*q^*\right] = -\frac{\partial}{\partial y}\left[v^*u^*\right] + \left[\frac{\partial}{\partial p}\left(\frac{1}{\sigma}\frac{\partial\Phi^*}{\partial x}\frac{\partial\Phi^*}{\partial p}\right) - \frac{1}{2\sigma}\frac{\partial}{\partial x}\left(\frac{\partial\Phi^*}{\partial p}\right)^2\right], \tag{9}$$

so that

$$\left[v^*q^*\right] = -\frac{\partial}{\partial y}\left[v^*u^*\right] + \left[\frac{\partial}{\partial p}\left(\frac{1}{\sigma}\frac{\partial\Phi^*}{\partial x}\frac{\partial\Phi^*}{\partial p}\right)\right]. \tag{10}$$

With (2) we obtain the final result (eq. 11.82):

$$\left[v^*q^*\right] = -\frac{\partial}{\partial y}\left[u^*v^*\right] + \frac{\partial}{\partial p}\left[f_0 v^*\left(\frac{1}{\sigma}\frac{\partial\Phi^*}{\partial p}\right)\right]. \tag{12}$$

we may state that

$$\frac{1}{\sigma}\frac{\partial\Phi^*}{\partial p} = -\frac{1}{S_p}T^*,$$

so that (11.82) becomes

$$\left[v^*q^*\right] = -\frac{\partial}{\partial y}\left[u^*v^*\right] - \frac{\partial}{\partial p}\left(\frac{f_0}{S_p}\left[v^*T^*\right]\right) = \vec{\nabla}\cdot\vec{F}. \tag{11.83}$$

This important equation was first derived by John Green (1970)[12]. Eq. 11.83 states that the divergence of the EP-flux vector is identical to an eddy flux of potential vorticity. **EP-flux divergence can be interpreted both as a force per unit mass and as a meridional flux of potential vorticity** (eqs. 11.66 and 11.83). Although the interpretation of EP-flux divergence as a force (manifest as "wave-drag" in the stratosphere) is very useful, as we shall see in chapter 12, the interpretation of EP-flux divergence as a meridional flux of potential vorticity is dynamically more fundamental. In an atmosphere, which is in thermal wind balance, potential vorticity is "connected" to the wind by "PV-inversion" (**Box 11.1** and chapter 7). Therefore, because non-zero EP flux divergence alters the zonal mean potential vorticity, it must also alter the zonal mean zonal wind in an atmosphere, which strives towards thermal wind balance.

Under not too restrictive circumstances, there exists a straightforward relation between the zonal mean meridional eddy flux of momentum and the zonal mean meridional eddy flux of absolute vorticity. Neglecting the spherical geometry of the Earth and assuming nondivergent isentropic flow, the eddy meridional flux of vorticity is

$$\zeta_a^*v^* = \zeta^*v^* = \left(\frac{\partial v^*}{\partial x} - \frac{\partial u^*}{\partial y}\right)v^* = \frac{1}{2}\frac{\partial v^{*2}}{\partial x} + u^*\frac{\partial v^*}{\partial y} - \frac{\partial u^*v^*}{\partial y} = \frac{1}{2}\frac{\partial v^{*2}}{\partial x} - \frac{1}{2}\frac{\partial u^{*2}}{\partial x} - \frac{\partial u^*v^*}{\partial y}$$

[12] See eq. (9) in Green, J.S.A., 1970: Transfer properties of the large scale eddies and the general circulation of the atmosphere. **Quart.J.R.Met.Soc., 96**, 157-185.

Averaging this expression over a latitude circle yields

$$\left[\zeta^* v^*\right] = -\frac{\partial\left[u^* v^*\right]}{\partial y}. \tag{11.84}$$

This means that

$$\left[v^* q^*\right] = \vec{\nabla}\cdot\vec{F} = \left[\zeta^* v^*\right] - \frac{\partial}{\partial p}\left(\frac{f_0}{S_p}\left[v^* T^*\right]\right) \tag{11.85}$$

The last term on the r.h.s. of eq. 11.85 represents the contribution of the eddies to the flux of mass. This can be seen by writing the above equation, using eq. 11.62, as follow.

$$\left[v^* q^*\right] = \left[\zeta^* v^*\right] - \frac{\partial}{\partial p}\left(\frac{f_0}{S_p}\left[v^* T^*\right]\right) = \left[\zeta^* v^*\right] - f_0\left(\left[v_a\right]_r - \left[v_a\right]\right) \tag{11.86}$$

The term, $f_0\left(\left[v_a\right]_r - \left[v_a\right]\right)$, is proportional to the **meridional poleward eddy flux of mass**. Therefore, eq. 11.86 reveals that an *equatorward* eddy flux of quasi-geostrophic potential vorticity ($\left[v^* q^*\right]<0$), which leads to a reduction of quasi-geostrophic potential vorticity over the polar cap, is associated with an *equatorward* eddy flux of quasi-geostrophic vorticity ($\left[\zeta^* v^*\right]<0$) and/or a *poleward* eddy flux of mass $f_0\left(\left[v_a\right]_r - \left[v_a\right]\right)>0$. This is consistent with the fact that a negative polar cap potential vorticity anomaly should coincide with a negative vorticity anomaly and a positive mass anomaly (**section 7.5**).

Let us imagine a region in the upper troposphere in the middle latitudes of the northern hemisphere, where $\vec{\nabla}\cdot\vec{F} < 0$, i.e. a region where the meridional flux of potential vorticity is negative (eq. 11.83), which implies an equatorward flux in the northern hemisphere. Let us assume that this *equatorward* flux of potential vorticity is maximized at a latitude of, say, 45°. On the **poleward side** of this latitude eq. 11.77 becomes (using eq. 11.83)

$$\frac{\partial\left[q\right]}{\partial t} = -\frac{\partial}{\partial y}\vec{\nabla}\cdot\vec{F} < 0, \tag{11.87a}$$

while on the **equatorward side** of this latitude we have

$$\frac{\partial\left[q\right]}{\partial t} = -\frac{\partial}{\partial y}\vec{\nabla}\cdot\vec{F} > 0. \tag{11.87b}$$

This will lead to a reduction of the meridional PV-gradient, i.e. a *negative* zonal mean PV-anomaly poleward of a *positive* zonal mean PV-anomaly. This is observed almost permanently in the lower stratosphere, between p=100 hPa and p=50 hPa, or between θ=380 K and θ=550 K in the northern hemisphere winter (**figure 7.7**). This layer is is referred as the "**surf-zone**". From what we have learned about the character of the solution the PV-inversion equation (chapter 7) we may tentatively conclude that the reduced meridional PV-gradient in the surf zone will translate into a reduced zonal mean zonal geostrophic wind in the surf zone. In other words the equatorward meridional flux of PV, due to the action of

planetary waves, leads to a *reduction* of the eastward zonal mean geostrophic zonal wind. It is as if eddies exert a drag on the zonal mean flow. Hence the term "planetary wave drag" is used as a powerful metaphor in our communication about the influence of zonal asymmetries on the zonal mean zonal geostropic wind.

Normally, the EP-flux vectors point upwards and dominantly towards the equator [13]. However, sometimes EP-flux vectors tend to converge towards the polar stratosphere. Anomalously convergence of EP-flux vectors over the polar stratosphere, which is associated with an anomalous equatorward flux of PV, is associated with the occurrence of Sudden Stratospheric Warmings (SSW) (**section 1.28**) in which the cyclonic polar vortex is destroyed and replaced by an anticyclonic polar vortex.

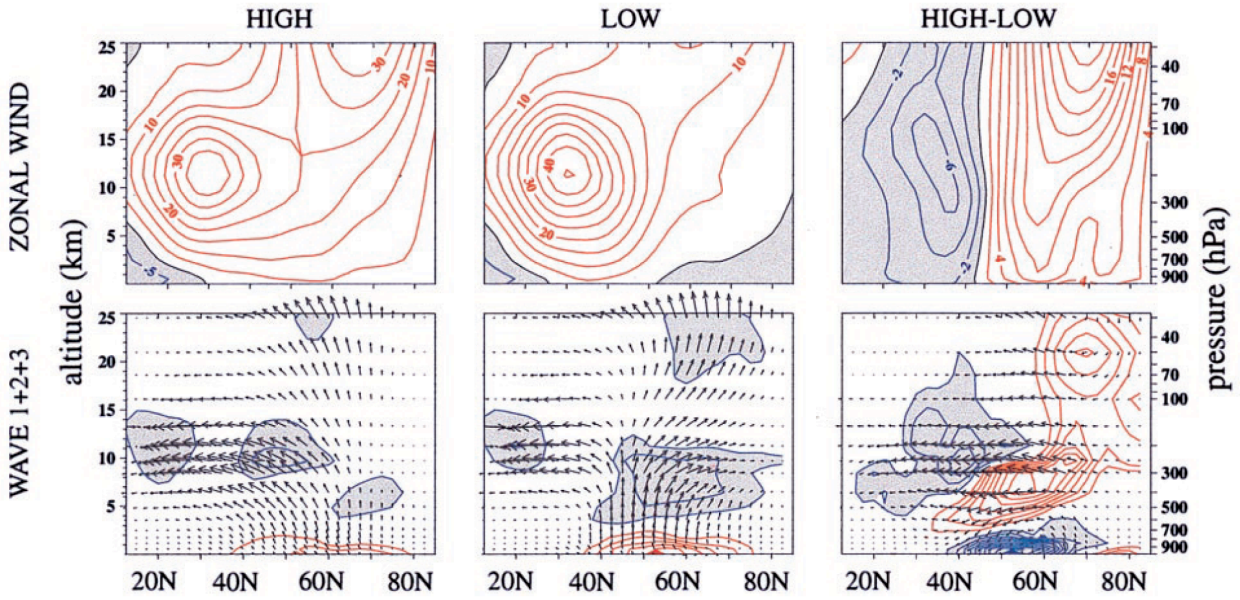

FIGURE 11.15. Composites for periods of high and low Northern Annular Mode (NAM)-index and their difference (left, centre and right) during the December to March period. Upper panels: zonal wind composites. Red contours correspond to positive values of [*u*]. Lower panels: EP-fluxes and their divergence for the sum of zonal wave numbers 1 to 3. Red contours correspond to positive values of EP-flux divergence. Source: Hartmann, D.L. J.M. Wallace, V Limpasuvan, D.W.J.Thompson and J.R. Holton, 2000. Can ozone depletion and global warming interact to produce rapid climate change? **PNAS, 97**, 1412-1417.

A clear relation exists between the meridional direction of EP-flux vectors and the Northern Annular Mode (NAM)[14] (**figure 11.15**). During the negative phase of the NAM, when sea level pressure is anomalously high over the Pole and anomalously low in the subtropics, EP-fluxes are directed more strongly toward the North Pole than during the positive phase of the NAM. This is consistent with the observation that SSW's occur more often during the negative NAM-phase. During a high positive phase of the NAM, Rossby waves seem to propagate into the subtropical jet, i.e. EP fluxes emanating from the middle latitudes are directed upward and equatorward, thus weakening the jet by planetary wave drag. Consistent with this we observe (**figure 11.15**) that the composite subtropical jet in the high positive NAM-phase is weaker than the composite subtropical jet in the low negative NAM-phase.

[13] See McIntyre (1982) and McIntyre and Palmer (1982) in the list of articles at the end of this chapter.

[14] See section 1.27 for a description of the Northern Annular Mode.

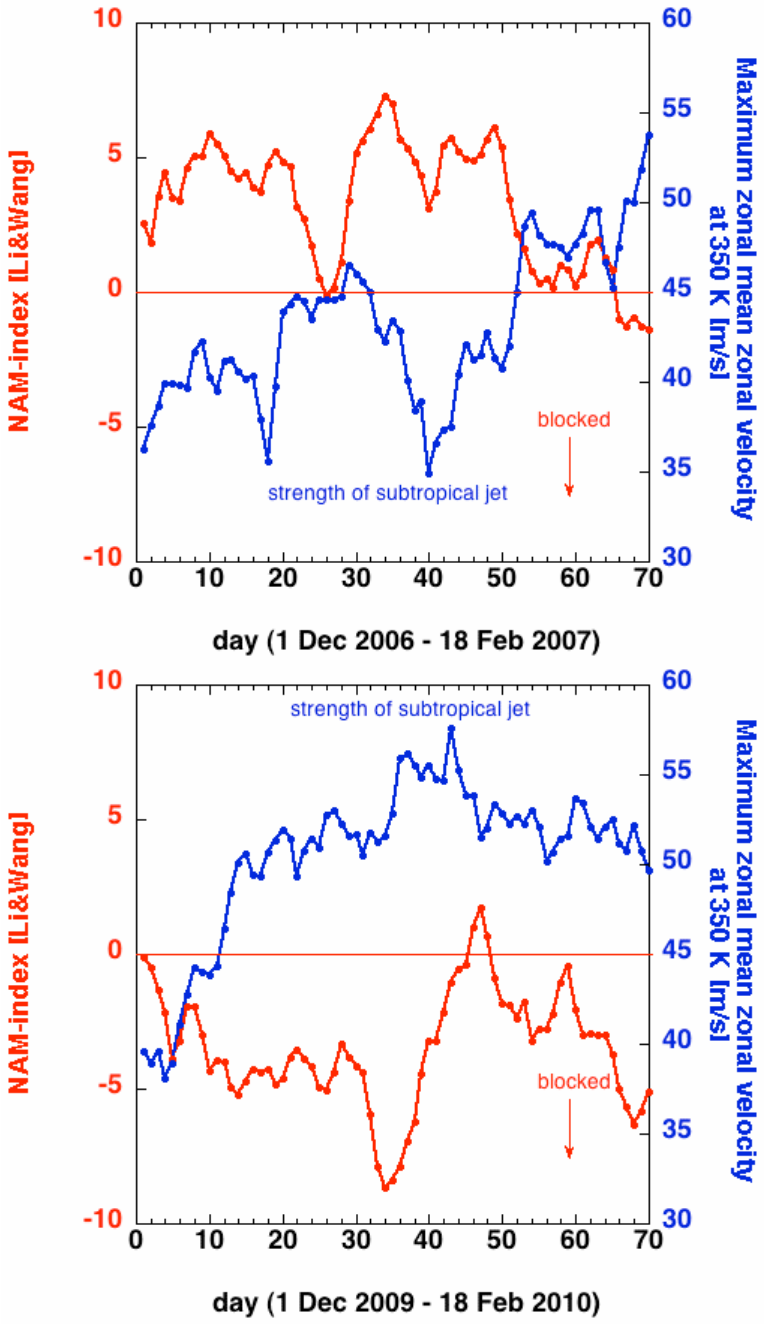

FIGURE 11.16. Maximum value of the daily mean zonal mean zonal wind in the subtropics at θ=350 K (blue line) and the daily mean NAM-index (according to the definition of Li and Wang; see section 1.27) during the winters of 2006-2007 (upper panel) and 2009-2010 (lower panel). Negative values of the NAM index are usually associated with appearance of "blocking" anticyclones at high latitudes, especially over Scandinavia and Alaska). Wind data are based on the 6-hourly ERA-Interim reanalysis (http://data-portal.ecmwf.int/data/d/interim_full_daily).

Figure 11.16 illustrates the remarkably strong negative correlation, even on the time scale of days, between the strength of the subtropical jet and the NAM-index. The theory, described in section 11.3, indicates that upward propagation of Rossby waves is hindered when the eastward zonal mean zonal wind velocity exceeds some critical value (eq. 11.17). In the light of this, we might hypothesize that upward and poleward propagation is preferred

during the negative phase of the NAM over upward and equatorward propagation (into the subtropical jet) because the zonal mean zonal wind velocity in the subtropical jet exceeds this critical value during this phase of the NAM. Moreover, this situation is advantageous for maintaining a strong subtropical jet and and will thus prolong the negative NAM-phase. This might explain the remarkably long time scale of the NAM (weeks to months), as is illustrated in **figure 11.16**.

PROBLEM 11.4. **Potential vorticity distribution in the winter polar vortex**

Using the ERA-Interim reanalysis data (http://apps.ecmwf.int/datasets/data/interim-full-moda/levtype=pt/), of monthly mean potential vorticity on θ=600 K, construct a covariance matrix of the zonal mean potential vorticity for this isentrope, similar to the covariance matrix due to Li and Wang (J. Li and J.X.L. Wang, 2003: A modified zonal index and its physical sense. **Geophys.Res.Lett., 30**, 1632) (http://ljp.gcess.cn/dct/page/65607). Define an index, which is a measure of a coherent extra-tropical oscillation in zonal mean potential vorticity on this isentrope, similar to the oscillation in sea level pressure that was identified by Li and Wang, leading to their definition of the sea-level NAM-index. What physical processes does this index reflect? Investigate the relation between the monthly NAM-index of Li and Wang and your index for the northern hemisphere winters of 2006-2007 and 2009-2010.

PROBLEM 11.5. **The major Sudden Stratospheric Warmings of the winters of 1984-1985, 2008-2009 and 2017-2018**

Based on the ERA-Interim reanalysis (http://apps.ecmwf.int/datasets/data/interim-full-daily/levtype=pl/), compute both components of the EP-flux vector (every 6 hours) at 100 hPa averaged over the latitudes, 40-80°N (a measure of the intensity of middle-latitude planetary wave propagation into the stratosphere and towards the pole) and investigate its relation with the **major stratospheric warmings (SSW)** of January 1985, January 2009 and February 2018. The SSW is reflected in the average temperature and in the average potential vorticity over the polar cap (north of 60°N) at 10 hPa, and also in the zonal mean zonal wind at 60°N.

PROBLEM 11.6. **Northern Annular Mode during the winters of 2006-2007 and 2009-2010**

Investigate the relation between both components of the EP-flux vector at 100 hPa at 60°N, during the winters of 2006-2007 and 2009-2010 and the daily mean NAM-index of Li and Wang (**problem 11.4**). Make a graph of both quantities. Discuss the characteristics of these two northern hemisphere winters. Interpret your result.

PROBLEM 11.7. Cold tropical tropopause

Temperatures at the tropical tropopause at about 100 hPa, which are approximately the lowest measured anywhere below the stratopause (**figure 12.1**), exhibit a yearly cycle with lowest values observed in January or February and highest values observed in July or August. Demonstrate this by constructing a Hovemoller plot of the zonal mean, monthly mean temperature at 100 hPa for the years 1979-2015, based on the ERA-Interim reanalysis (http://apps.ecmwf.int/datasets/data/interim-full-daily/levtype=pl/). Explain the yearly cycle (see the paper by Yulaeva et al., 1994, listed at the end of chapter 12) and investigate trends in the data.

ABSTRACT OF CHAPTER 11

Chapter 11 introduces the **quasi-geostrophic potential vorticity**, the **index of refraction** for Rossby wave propagation in the meridional plane, the **Eliassen-Palm flux** (as a diagnostic of the effect of vertical and meridional planetary wave propagation on the zonal mean zonal flow), the idea that waves may induce both an acceleration and a deceleration of the zonal mean zonal flow (in the latter case this effect of waves on the zonal mean zonal wind is referred to as **planetary wave drag**), the Eulerian mean circulation as a model of the well-known mid-latitude **Ferrel circulation** and the **transformed Eulerian mean meridional circulation** as a model of the actual net meridional (zonal-averaged) flux of heat and other conserved quantities. The latter model appears to be useful when diabatic response to wave drag is taken into account, in which case the lagrangian meridional circulation is interpreted as the "**diabatic circulation**".

Assuming that the **zonal mean atmosphere remains in thermal wind balance** at all times yields an equation for the zonal mean meridional circulation (the **Kuo-Eliassen equation**). The Eulerian version of this equation describes the **Ferrel circulation**. Its solution reveals that the Ferrel circulation is forced by eddy meridional fluxes of heat and momentum and by diabatic heating. The "transformed Eulerian" version of this equation describes the **Brewer-Dobson circulation** and, thus, encompasses the meridional transport of mass by eddies. The solution of this equation reveals that the meridional circulation of mass is upward in the tropics and downward in over the Polar cap. Therefore, air is cooled adiabatically in the tropics and is heated adiabatically over the poles. This explains the existence of the **cold point tropical tropopause**.

Finally, it is shown that the divergence of the Eliassen-Palm flux can be identified with the **isobaric eddy meridional flux of quasi-geostrophic potential vorticity**. This interpretation of the effect of waves on the zonal mean state of the atmosphere, which is probably more fundamental than the interpretation in terms of wave drag, will be elaborated upon further in chapter 12.

Further reading

Books

Wallace, J.M. and P.V. Hobbs, 2006: **Atmospheric Science: An Introductory Survey**. Academis Press, 483 pp.

James, I.N., 1994: **Introduction to Circulating Atmospheres**. Cambridge University press, 422 pp. (Chapter 6)

Vallis, G.K., 2006: **Atmospheric and Oceanic Fluid Dynamics**. Cambridge University Press. 745 pp. (Chapter 7)

Holton, J.R., 2004. **An Introduction to Dynamic Meteorology**. Academic Press. (Chapter 10)

Articles

Butchart, N., 2014: The Brewer-Dobson circulation, **Rev. Geophys., 52,** 157–184, doi:10.1002/2013RG000448.

Edmon, Jr., H.J., B.J. Hoskins and M.E. McIntyre, 1980: Eliassen-Palm cross sections for the troposphere. . **J.Atmos.Sci., 37**, 2600-2616.

Hartmann, D.L., 2007: The atmospheric general circulation and its variability. **J.Meteorol.Soc.Japan, 85B**, 123-143.

Haynes, P., 2005: Stratospheric Dynamics. **Ann.Rev.Fluid Mechanics, 37**, 263-293.

Holton, J.R., 1980: The dnamics of sudden stratospheric warmings. **Ann.Rev.Earth Plan. Sci., 8**, 169-190.

Holton, J.R., P.H. Haynes, M.E. McIntyre, A.R. Douglass, R.B. Rood and L. Pfister, 1995: Stratosphere-troposphere exchange. **Rev.Geophys., 33**, 403-439.

McIntyre, M.E.,, and T.N. Palmer, 1982: Breaking planetary waves in the stratosphere. **Nature, 305**, 593-600.

McIntyre, M.E., 1982: How well do we understand the dynamics of sudden stratospheric warmings? **J.Meteorol.Soc.Japan, 60**, 37-65.

Shepherd, T.G, 2002: Issues in stratosphere-troposphere coupling. **J.Meteorol.Soc.Japan, 80**, 769-792.

Shepherd, T.G., 2003: Large-scale atmospheric dynamics for atmospheric chemists. **Chem.Rev., 103**, 4509-4531.

List of problems (chapter 11)

This is the April 2020 edition of chapter 11 (first written in December 2012) of the lecture notes on Atmospheric Dynamics, by Aarnout van Delden (IMAU, Utrecht University, Netherlands, a.j.vandelden@uu.nl).
http://www.staff.science.uu.nl/~delde102/AtmosphericDynamics.htm